

Manuscript prepared for Atmos. Chem. Phys.
 with version 2014/09/16 7.15 Copernicus papers of the L^AT_EX class copernicus.cls.
 Date: 24 February 2015

Chemical aging of single and multicomponent biomass burning aerosol surrogate-particles by OH: Implications for cloud condensation nucleus activity

J. H. Slade¹, R. Thalman², J. Wang², and D. A. Knopf¹

¹State University of New York at Stony Brook, School of Marine and Atmospheric Sciences, Stony Brook, NY 11374

²Brookhaven National Laboratory, Department of Environmental and Climate Sciences, Upton, NY 11973

Correspondence to: Daniel A. Knopf (Daniel.Knopf@StonyBrook.edu)

Abstract. Multiphase OH and O₃ oxidation reactions with atmospheric organic aerosol (OA) can influence particle physicochemical properties including composition, morphology, and lifetime. Chemical aging of initially insoluble or low soluble single-component OA by OH and O₃ can increase their water-solubility and hygroscopicity, making them more active as cloud condensation nuclei (CCN) and susceptible to wet deposition. However, an outstanding problem is whether the effects of chemical aging on their CCN activity is preserved when mixed with other organic or inorganic compounds exhibiting greater water-solubility. In this work, the CCN activity of laboratory-generated biomass burning aerosol (BBA) surrogate-particles exposed to OH and O₃ is evaluated by determining the hygroscopicity parameter, κ , as a function of particle type, mixing state, and OH/O₃ exposure applying a CCN counter (CCNc) coupled to an aerosol flow reactor (AFR). Levoglucosan (LEV), 4-methyl-5-nitrocatechol (MNC), and potassium sulfate (KS) serve as representative BBA compounds that exhibit different hygroscopicity, water solubility, chemical functionalities, and reactivity with OH radicals, and thus exemplify the complexity of mixed inorganic/organic aerosol in the atmosphere. The CCN activities of all of the particles were unaffected by O₃ exposure. Following exposure to OH, κ of MNC was enhanced by an order of magnitude, from 0.009 to ~ 0.1 , indicating that chemically-aged MNC particles are better CCN and more prone to wet deposition than pure MNC particles. No significant enhancement in κ was observed for pure LEV particles following OH exposure. κ of the internally-mixed particles was not affected by OH oxidation. Furthermore, the CCN activity of OH exposed MNC-coated KS particles is similar to the OH unexposed atomized 1:1 by mass MNC:KS binary-component particles. Our results strongly suggest that when OA is dominated by water-soluble organic carbon (WSOC) or inorganic ions, chemical aging has no sig-

nificant impact on OA hygroscopicity. The organic compounds exhibiting low solubility behave as if they are infinitely soluble when mixed with a sufficient amount of water-soluble compounds. At and beyond this point, the particles' CCN activity is governed entirely by the water-soluble fraction and not influenced by the oxidized organic fraction. Our results have important implications for heterogeneous oxidation and its impact on cloud formation given that atmospheric aerosol is a complex mixture of organic and inorganic compounds exhibiting a wide-range of solubilities.

1 Introduction

The extent that aerosol-cloud interactions impact the atmospheric radiative budget and climate change is significant, but remains highly uncertain (Stocker et al., 2013). Attributed to this uncertainty is the difficulty to quantify the effects of chemical aging during atmospheric particle transport by heterogeneous or multiphase chemical reactions between organic aerosol particles and trace gas-phase oxidants and radicals (Abbatt et al., 2012; Pöschl, 2011; George and Abbatt, 2010; Rudich et al., 2007). Heterogeneous oxidation reactions between organic aerosol particles and OH, O₃, or NO₃ can impact the particles' physical and chemical properties (Ellison et al., 1999; Rudich, 2003; Pöschl, 2005; Rudich et al., 2007; George and Abbatt, 2010), and has been shown to impact particle hygroscopicity and cloud condensation nuclei (CCN) activity (Broekhuizen et al., 2004; Petters et al., 2006; Shilling et al., 2007; Pöschl, 2011; George et al., 2009) and ice nucleation (IN) (Wang and Knopf, 2011; Brooks et al., 2014).

Cloud nucleation efficiency depends on the particle's solubility in water and hygroscopicity (Petters and Kreidenweis, 2007, 2008), and particle size (Dusek et al., 2006) and morphology (Giordano et al., 2014). The majority of submicron aerosol particles are comprised of organic material (Zhang et al., 2007; Hallquist et al., 2009), which possess a wide range of hygroscopicity ($\kappa \sim 0.01-0.5$) (Petters and Kreidenweis, 2007). A significant portion of atmospheric organic aerosol (OA) is derived from biomass burning (BB) emissions (Bond et al., 2004; Andreae et al., 2004; Hays et al., 2005; Monks et al., 2009). BB plays an important role both regionally and globally (Park et al., 2007), accounting for an estimated 2.5 Pg C yr⁻¹ (van der Werf et al., 2006). Reflectance data from satellite retrievals indicate that BB accounts for a global footprint of 464 Mha yr⁻¹ or roughly ~36% of cropland on earth (Randerson et al., 2012). Biomass burning aerosol (BBA) constitutes a significant fraction of primary organic aerosol (POA) (Bond et al., 2004) and secondary organic aerosol (SOA), derived from oxidative aging of volatile and semi-volatile organic vapors emitted from biomass burning plumes (Carrico et al., 2010; Hallquist et al., 2009; Jathar et al., 2014). Molecular markers of BB POA include pyrolyzed forms of glucose such as levoglucosan (LEV, 1-6-anhydro- β -glucopyranose) (Simoneit, 1999) and potassium containing salts such as potassium sulfate (KS, K₂SO₄) (Sheffield et al., 1994). The photo-oxidation of *m*-cresol, which is emitted at high levels from biomass burning (Schauer et al., 2001), in the presence of NO_x, generates 4-methyl-5-nitrocatechol (MNC), which has

recently been recognized as a potentially important tracer for biomass burning SOA (Iinuma et al., 2010). With the exception of MNC, the CCN activity and hygroscopicity of LEV and KS, among other select BBA compounds and smoke particles, have been determined (Petters et al., 2009; Carrico et al., 2010). Dusek et al. (2011) measured κ values of 0.2 for the water-soluble organic content (WSOC) in particles produced from controlled laboratory burns. Carrico et al. (2010) determined a mean κ of 0.1 for carbonaceous particles sampled from open combustion of several biomass fuels. Hygroscopic growth factors of levoglucosan and other biomass burning derived organics range from 1.27-1.29 at RH=90% (Chan et al., 2005; Mikhailov et al., 2009). In-situ field measurements of the CCN efficiency (ratio of CCN to the available condensation nuclei, CN) of biomass burning smoke particles is on the order of 50% at 1% supersaturation (Andreae et al., 2004). While inorganic ions have only a minor importance as an atmospheric tracer for biomass burning, they can significantly influence the CCN activity of BBA, even if their fractions are significantly less than the organic fraction (Iinuma et al., 2007; Roberts et al., 2002)

Heterogeneous OH oxidation of organic aerosol can initiate reactions that result in the production of oxidized polar functional groups that can reduce the particle's surface tension (George et al., 2009) and increase water-solubility (Suda et al., 2014), enabling greater water uptake and CCN activity. For example, Broekhuizen et al. (2004) demonstrated that unsaturated fatty acid aerosol particles comprised of oleic acid became more CCN active in the presence of high exposures to O₃. In a follow-up study, Shilling et al. (2007) corroborated this finding, attributing the enhancement in CCN activity to a combination of an increase in water-soluble material and decrease in surface tension of the aqueous droplet during activation. Petters et al. (2006) demonstrated that the CCN activity of model saturated and unsaturated OA compounds is enhanced following oxidation by OH and NO₃. George et al. (2009) showed that the hygroscopicity of a model OA, bis-ethyl-sebacate (BES) and stearic acid, was enhanced following oxidative aging by OH radicals, and attributed this to the formation of highly water-soluble oxygenated functional groups. The hygroscopicity of OH-impacted ambient biogenic SOA was shown to increase at higher OH exposures with increasing oxygen-to-carbon (O:C) ratio (Wong et al., 2011).

In an effort to better understand the influence of chemical aging on the CCN activity of BBA, recent studies have investigated the influence of oxidative aging on particle hygroscopicity of either particles generated in the laboratory from a specific emission source (Martin et al., 2013; Grieshop et al., 2009; Novakov and Corrigan, 1996) or particles collected in the field (Rose et al., 2010; Gunthe et al., 2009), which may include multiple emission sources. While field-collected particle studies of hygroscopic growth and cloud formation are advantageous because they capture the chemical and physical complexity of ambient aerosol, they lack the specificity and control of laboratory studies in order to fully understand the fundamental physico-chemical processes that govern cloud formation. Martin et al. (2013) investigated the impact of photo-oxidation on the hygroscopicity of wood burning particles and found that after several hours of aging in a smog chamber there is a general

enhancement in κ ; however, this was attributed to sequential condensation of oxidized organic or
95 inorganic matter and oxidation of the particulate matter itself. However, the effects of OH-initiated
oxidation on the hygroscopicity of BBA particles have yet not been examined systematically. In
this work, we investigate the effects of heterogeneous OH oxidation of laboratory-generated BBA
surrogate-particles on the particles' hygroscopicity. Here, κ is evaluated for several pure-component
and multicomponent aerosol particles containing both sparingly soluble and highly water-soluble
100 compounds, representing the range and complexity of atmospheric aerosol in regards to hygroscopic-
ity and chemical composition. κ is evaluated as a function of OH exposure (i.e. $[\text{OH}] \times \text{time}$) and
 O_3 exposure using a custom-built AFR coupled to CCNc. The effects of chemical aging on the CCN
activity of internally mixed and organic-coated inorganic particles are presented.

2 Materials and Methods

2.1 Aerosol generation, flow conditions, and measurement

Surrogate polydisperse BBA particles were generated by atomizing 1 wt. % aqueous solutions of
single-component particles LEV, MNC, KS, and particle mixtures of LEV:MNC:KS in 1:1:0, 0:1:1,
1:0:1, 1:1:1, and 1:0.03:0.3 mass ratios in a flow of ultra-high purity (UHP) N_2 using a commercial
atomizer (TSI, Inc. model 3076). To simulate the partitioning of MNC from the gas phase to the
110 particulate phase, first reagent MNC was heated (up to $\sim 70^\circ\text{C}$) and volatilized, and then condensed
onto KS seed particles. Growth of the KS seed particles by MNC condensation was achieved by
gradually cooling the mixed MNC/KS flow downstream of the heating section before entering the
flow reactor. The atomized particles were dried by passing the atomized flow through two diffusion
dryers prior to entering the AFR. After exiting the AFR, the particles were subsequently dried in
115 two additional diffusion dryers, where the overall sample flow $\text{RH} \leq 5\%$, before the size analysis and
CCN activity measurements. The dry particle size distribution was determined with a differential
mobility analyzer (DMA, TSI Inc. model 3081) and condensation particle counter (CPC, TSI Inc.
model 3772), and sampled at a total flow rate of 1.3 standard liters per minute (slpm). Number-
weighted mean particle diameters, \overline{D}_p , for all of the particles investigated in this study ranged from
120 ~ 40 -150 nm.

2.2 OH generation, flow conditions, and measurement

OH radicals were generated via O_3 photolysis in the presence of water vapor in a 60 cm in length
and 5 cm i.d. temperature-controlled Pyrex flow reactor as shown in Fig. 1 (Slade and Knopf, 2013;
Kessler et al., 2010; George et al., 2009). O_3 was produced by flowing 2-25 sccm (standard cubic
125 centimeters per minute) of UHP O_2 through an O_3 producing lamp (Jelight model 600; emission
wavelength, $\lambda=185$ nm). O_3 concentrations ranged between 250 ppb and 20 ppm and were moni-
tored throughout the experiment using an O_3 photometric analyzer (2B Technologies model 202),

which sampled at ~ 850 sccm. An O_3 denuder containing Carulite 200 catalyst was connected to the outlet of the AFR to convert O_3 to O_2 before entering the aerosol charge neutralizer and other sensitive instrumentation. A 50-600 sccm flow of UHP N_2 was bubbled in a 500 mL Erlenmeyer flask filled with distilled/deionized Millipore water (resistivity >18.2 M Ω cm) to generate humidified conditions in the AFR, where the relative humidity (RH) for all of the experiments varied from 30% to 45% determined by an RH probe (Vaisala model HM70). The humidified and O_3 flows were mixed in a 4.5 L glass vessel before entering with the particles into the AFR. The mixed $N_2/O_2/O_3/H_2O$ and particle flow was then passed over a 60 cm O_3 -free quartz tube containing a 60 cm length mercury pen-ray lamp ($\lambda > 220$ nm) to photolyze O_3 . The lamp was cooled with a flow of compressed air. Total flow rates in the flow reactor ranged from ~ 2.2 -3 slpm corresponding to a range in residence times of 26-39 s. Flows were laminar with Reynold's numbers between 60 and 80. OH concentrations were determined applying a photochemical box model validated based on isoprene loss measurements in the presence of OH as described previously (Slade and Knopf, 2013; George et al., 2009). OH concentrations ranged from $\sim 0.2 \times 10^{10}$ - 2×10^{10} molecule cm^{-3} and were varied by changing either RH or $[O_3]$. As previous studies have indicated, neither UV light nor O_3 introduction in this manner leads to particle degradation or a significant change in particle mass or chemistry (George et al., 2009; Kessler et al., 2010; Slade and Knopf, 2013). Temperature inside the flow reactor was maintained near 298 K by a cooling jacket. A slight temperature gradient of $\sim 3^\circ C$ from the leading edge of the sheath flow tube containing the lamp to the inner walls of the AFR was observed, but has no significant effect on [OH]. OH equivalent atmospheric exposures were determined from the product of the residence time in the AFR and applied [OH], which was then normalized to a daily averaged ambient $[OH] = 2 \times 10^6$ molecule cm^{-3} . Using this method allowed varying atmospheric OH exposures equivalent to <1 day up to ~ 1 week. At the given [OH], residence time, total pressure of 1 atm, and particle sizes, we assume OH mass transfer to the particles is sufficiently fast to maximize the exposure. At 40% RH, the reactive uptake coefficient, γ , of LEV+OH would be 0.65 for atmospheric OH concentrations (Slade and Knopf, 2014). However, the presence of higher [OH] in the AFR decreases γ to ~ 0.2 (Slade and Knopf, 2013). OH diffusion impacts γ by only $\sim 7\%$ (Fuchs and Sutugin, 1970) implying that OH exposure is not diffusion limited. At RH $> 15\%$, MNC is less reactive with OH, exhibiting $\gamma < 0.07$ due to competitive co-adsorption of water and OH (Slade and Knopf, 2014). The presence of higher $[O_3]$ may further decrease the OH reactivity of OA (Renbaum and Smith, 2011). Under the applied experimental conditions, the multiphase reaction kinetics involving highly viscous organic material are likely limited by surface-bulk exchange (Arangio et al., 2014; Slade and Knopf, 2014).

2.3 CCN Measurements

The CCNc and operating conditions are described in more detail in Mei et al. (2013a). CCN activity data were acquired following procedures similar to previous studies (Petters and Kreidenweis, 2007;

Petters et al., 2009), whereby the dry particle diameter is scanned while keeping the CCN chamber supersaturation fixed. A more detailed description of this approach is given in Petters et al. (2009). Briefly, particles first passed through a Kr-85 aerosol neutralizer (TSI 3077A) were size-selected using a DMA (TSI 3081) and processed in a CCNc (DMT, single column CCNc) (Roberts and Nenes, 2005; Lance et al., 2006; Rose et al., 2008), while in tandem the total particle concentration was measured with a CPC. The CCNc was operated at 0.3 slpm total flow rate and 10:1 sheath-to-sample flow rate ratio. The total sample flow rate, which includes a 1 slpm CPC flow rate was 1.3 slpm and 10:1.3 sheath-to-sample flow rate ratio was applied for the DMA. The temperature gradient in the CCNc column was set by custom-programmed Labview software and operated at $\Delta T=6.5, 8, 10, \text{ and } 12 \text{ K}$, corresponding to chamber supersaturations $S=0.2, 0.27, 0.35, \text{ and } 0.425\%$ based on routine calibrations applying atomized ammonium sulfate particles. The temperature gradient was stepped successively, from 6.5-12 K and in reverse. Each temperature gradient was maintained for a total of 14 min to allow an up and down scan of the particle size distribution by the DMA. The aerosol size distributions and size-resolved CCN concentrations were acquired applying an inversion method described in Collins et al. (2002), which implicitly accounts for multiply charged particles. The ratio of the aerosol size distribution and CCN size distribution provided size-resolved CCN activated fractions (i.e. fraction of particles that become CCN at a given supersaturation and particle size).

2.4 Hygroscopicity and CCN Activity Determination

The hygroscopicity and CCN activity can be described by κ -Köhler theory (Petters and Kreidenweis, 2007), which relates dry and wet particle diameter to the particle's critical supersaturation (RH above 100% at which the particle grows to a cloud droplet size) based on a single hygroscopicity parameter, κ . In κ -Köhler theory, the water vapor saturation ratio over an aqueous solution droplet as a function of droplet diameter, $S(D)$, is given by

$$S(D) = \frac{D^3 - D_d^3}{D^3 - D_d^3(1 - \kappa)} \exp\left(\frac{4\sigma M_w}{RT\rho_w D}\right), \quad (1)$$

where D is wet particle diameter, D_d is dry particle diameter, σ is droplet surface tension, M_w is the molecular weight of water, R is the universal gas constant, T is temperature, and ρ_w is density of water. κ ranges typically from ~ 0.5 -1.4 for hygroscopic inorganic species and from ~ 0.01 -0.5 for less-hygroscopic organic species; $\kappa=0$ represents an insoluble but wettable particle and thus Eq. 1 reduces to the Kelvin equation (Petters and Kreidenweis, 2007).

An alternative, approximate expression for determining κ is given as follows (Petters and Kreidenweis, 2007):

$$\kappa = \frac{4A^3}{27D_d^3 \ln^2 S_c}, \quad (2)$$

where

$$A = \frac{4\sigma_{s/a}M_w}{RT\rho_w}. \quad (3)$$

S_c represents the critical supersaturation, i.e. point of supersaturation where more than 50% of the initial dry particles are activated to CCN.

Hygroscopic growth of compounds exhibiting moderate to weak solubility in water can be limited by their low water-solubility (Petters and Kreidenweis, 2008), and thus cannot be treated as either fully dissolvable or insoluble substances. A theoretical treatment of κ , which includes solubility limitations has been detailed in Petters and Kreidenweis (2008). Here,

$$\kappa = \varepsilon_i \kappa_i H(x_i) \quad (4)$$

$$H(x_i) = \begin{cases} 1 & \text{if } x_i \geq 1; \\ x_i & \text{if } x_i < 1. \end{cases},$$

where ε is the volume fraction of the solute i in the dry particle. κ_i is the theoretical κ of solute i in the absence of solubility limitations and given by

$$\kappa_i = \frac{\nu \rho_i m_w}{\rho_w m_i}, \quad (6)$$

where ν is the Van't Hoff factor, ρ_i is the density of solute, ρ_w is the density of water, m_i is the molar mass of the solute, and m_w is the molar mass of water. x_i is defined as the dissolved volume fraction of the solute (Petters and Kreidenweis, 2008) and given as

$$x_i = C_i \frac{V_w}{V_i}, \quad (7)$$

where C_i is the water solubility of the solute, expressed as the solute volume per unit water volume at equilibrium with saturation, and V_i is the volume of the solute. For complete dissociation, x_i is equal to unity. The parameters listed in table 1 were used in predicting κ .

3 Results and Discussion

3.1 CCN activity of BBA surrogate-particles

Exemplary activated fractions, i.e. fraction of initial dry particle sizes activated to CCN, for LEV, MNC, KS, and the ternary particle mixtures at a chamber supersaturation of 0.425% are shown in Fig. 2. The activated fraction curves were fit to a cumulative Gaussian distribution function as described previously in detail (Petters et al., 2009)

$$f(x) = \frac{1}{2} \operatorname{erfc}\left(\frac{x}{\sqrt{2}}\right), \quad (8)$$

225 where $x = (D_d - D_{d,50})/\sigma_D$. In the fitting procedure, D_d is the dependent variable and $D_{d,50}$ and σ_D are adjustable parameters to minimize the root mean square error between $f(x)$ and the data. $D_{d,50}$ is the dry diameter interpreted as where 50% of the dry particles have activated into cloud droplets, also referred to as the critical particle diameter, $D_{p,c}$.

230 KS particles exhibit the smallest particle activation diameter of ~ 50 nm, followed by LEV particles at ~ 75 nm, and MNC particles at ~ 210 nm at $S=0.425\%$. In this study, κ is derived from Eq. 2, where S evaluated at 0.2, 0.27, 0.35, and 0.425% is used in place of S_c and D_d is the determined $D_{p,c}$. At lower S , the activated fraction curves are shifted to larger sizes since the smaller particles do not activate at lower S .

235 Table 2 lists the derived κ values for all of the particle types employed in this study in comparison to literature values. The reported uncertainties in κ are $\pm 1\sigma$ from the mean κ measured at all S . The measured κ values for LEV and KS are consistent with κ for LEV and KS given in the literature. The critical diameter of LEV (~ 70 nm at $S=0.425\%$) is in good agreement with the critical diameter of LEV measured by Petters and Kreidenweis (2007) at the same S . $\kappa=0.169$ for LEV is close to the humidified tandem-DMA (HT-DMA) derived $\kappa=0.165$ (Carrico et al., 2010). Within experimental uncertainty, κ for KS is in agreement with the value derived in Carrico et al. (2010). To our knowledge, no previous hygroscopicity measurements of MNC have been made. For comparison, HULIS, which is known to contain nitrocatechols (Claeys et al., 2012), exhibits a κ value of 0.05 (Carrico et al., 2010). In addition, κ for NO_3 oxidized oleic acid particles, comprising similar chemical functionalities as MNC (i.e. nitrogen oxides and conjugated double bonds) is ~ 0.01 (Petters et al., 2006).

245 κ of the binary and ternary mixed particles, on average range from 0.131 (± 0.014) to 0.355 (± 0.042). The mixed particles containing a significant fraction of MNC (i.e. 1:1:0, 0:1:1, 1:1:1) exhibit relatively lower κ values than the 1:0:1 mixture. This is expected since MNC alone has significantly lower κ than either LEV or KS. The 1:0.03:0.3 ternary-component particles exhibit a slightly lower κ compared to the other particle mixtures, due to the relatively low KS content. As listed in table 2, the measured κ values are reasonably predicted applying the volume mixing rule (Petters and Kreidenweis, 2007):

$$\kappa = \kappa_{\text{Org}} \cdot \varepsilon_{\text{Org}} + \kappa_{\text{Inorg}}(1 - \varepsilon_{\text{Org}}), \quad (9)$$

255 where κ_{Org} and κ_{Inorg} are the κ values of the organic and inorganic particles, respectively, and ε_{Org} is the organic volume fraction of the particles. However, the quality of the estimate depends on whether the effects of solubility are to be included. For example, applying the experimentally-derived κ of MNC particles in the volume mixing rule results in a significant underprediction of κ for the 1:1:0, 0:1:1, and 1:1:1 particle mixtures. This deviation in κ suggests that water uptake by the pure-component MNC particles is mechanistically different than water uptake by the mixed particles, which contain significant amounts of MNC. The volume mixing rule is applicable over a range of mixtures and hygroscopicity; however, when the particles contain both soluble and spar-

ingly soluble compounds, predicted κ can deviate significantly from measured κ values (Petters and Kreidenweis, 2008). MNC is significantly less soluble in water compared to pure LEV and KS. During CCN activation, the most water-soluble material dissolves first and enhances the solute effect in the Köhler equation. More water-soluble particles retain a larger content of liquid water and consequently, the less water-soluble material can more easily dissolve in the presence of hygroscopic and water-soluble substances during water uptake (Bilde and Svenningsson, 2004; Abbatt et al., 2005; Shantz et al., 2008; Petters and Kreidenweis, 2008). This solubility constraint in the volume mixing rule is described in more detail in Petters and Kreidenweis (2008). As a result, depending on the volume fraction of the sparingly soluble compounds, the peak of the Köhler curve may occur at a sufficiently large droplet size when all compounds, including the sparingly soluble compounds, are completely dissolved. The same can be applied here for the mixtures containing appreciable amounts of MNC. The solubility of MNC in water is $C=0.004$ and falls in the sparingly water-soluble category (Petters and Kreidenweis, 2008). To verify whether MNC behaves as if it is infinitely soluble in a solution containing KS, Fig. 3 shows derived Köhler curves of pure MNC and mixtures containing variable amounts of KS, and the MNC dissolved fraction, x_{MNC} . According to Fig. 3, the critical supersaturation, i.e. maximum in the Köhler curve, decreases with increasing KS volume fraction. Accordingly, the dissolved fraction of MNC increases with increasing KS volume fraction. At a KS volume fraction of $\sim 36\%$ (MNC volume fraction of $\sim 64\%$) indicated by the orange curves in Fig. 3, the maximum in the Köhler curve corresponds to $x_{\text{MNC}} \approx 1$, implying that CCN activation is not limited by MNC solubility. This MNC volume fraction corresponds to the 1:1 by mass MNC:KS particles, which suggests that for this particular mixture, MNC behaves as if there are no solubility limitations (i.e. infinitely soluble) during CCN activation and κ of MNC can be predicted using Eq. 6. This result is consistent for both the 1:1 by mass LEV:MNC and 1:1:1 by mass LEV:MNC:KS particles. Figure 4 shows the predicted κ values including solubility constraints (open circles) and excluding solubility limitations (closed circles) plotted against the measured κ values for all of the particle mixtures applied in this study.

The measured κ for the 1:1 by mass MNC:KS is $0.301 (\pm 0.047)$. When including MNC solubility limitations, i.e. applying the experimentally derived κ of pure MNC in the volume mixing rule, the predicted κ of the mixture is significantly less at 0.204 (open blue circles in Fig. 4). However, when excluding the effects of solubility, predicted $\kappa=0.300$ (closed blue circles in Fig. 4), is in excellent agreement with the measured κ . Except for the 1:0.03:0.3 by mass LEV:MNC:KS particles (open purple circles in Fig. 4), the predicted κ values applying the volume mixing rule of 1:1 by mass LEV:MNC (open red circles) and 1:1:1 by mass LEV:MNC:KS (open green circles) particles are significantly lower than the experimentally derived κ . However, when excluding their solubility limitations, the predicted κ values are in much better agreement with the measurements. The volume content of MNC in the 1:0.03:0.3 by mass LEV:MNC:KS particles was too low to impact the measured κ values.

3.2 CCN activity of single-component BBA surrogate-particles exposed to OH and O₃

300 Surrogate single-component BBA particles were oxidized in the presence of O₃ (mixing ratio, χ_{O_3} =0.76-20 ppm) and in the presence of OH radicals (0.2×10^{10} - 2×10^{10} molecule cm⁻³), corresponding to <1 day up to ~ 1 week of a 12-hr daytime OH exposure at [OH] = 2×10^6 molecule cm⁻³ and <1 hr up to 10 hrs of O₃ exposure at a background χ_{O_3} =20 ppb (Vingarzan, 2004). The hygroscopicity of the particles was determined as a function of OH and O₃ exposure. The results for
305 the single-component organic particles LEV and MNC are shown in Fig. 5.

The reactive uptake, condensed-phase reaction products, and volatilized reaction products resulting from heterogeneous OH oxidation of LEV is well-documented (Kessler et al., 2010; Hoffmann et al., 2010; Bai et al., 2013; Slade and Knopf, 2013, 2014; Zhao et al., 2014). However, there are no direct measurements of its CCN activity following OH oxidation. Kessler et al. (2010) showed
310 that following OH exposure, particle volatilization accounts for a ~20% by mass loss of LEV. This suggests that the majority of the reaction products, which include carboxylic and aldehydic species (Bai et al., 2013; Zhao et al., 2014), remain in the condensed-phase. Although volatilization due to high OH exposures has been linked to an increase in the critical supersaturation and thus suppression in the CCN activity of oxidized squalane particles (Harmon et al., 2013), the results here suggest re-
315 gardless of volatilization, the condensed-phase reaction products are just as or somewhat more active CCN than pure LEV. On average, there is a slight increase in κ for LEV particles with increasing OH exposure as indicated by the positive slope in the linear fit to the data ($\kappa = 9 \times 10^{-15} \cdot [\text{OH}]_{\text{exp}} + 0.17$); however, this apparent enhancement in κ is not significant since the average κ values for each OH exposure fall well within the range of measured κ . Such an incremental enhancement in κ may be a
320 result of similar κ between LEV and its oxidation products. The hygroscopicity of several carboxylic acids that may represent OH oxidation products, including malonic, glutaric, glutamic, succinic, and adipic acid exhibit κ values between 0.088-0.248 (Petters and Kreidenweis, 2007), similar to κ of oxidized and pure LEV. Furthermore, the hygroscopicity of organic compounds containing hydroxyl functionalities (like LEV) or carboxylic groups are nearly equivalent (Suda et al., 2014). We also
325 cannot rule out that volatilization, while reducing particle mass, also removes newly formed reaction products from the aerosol phase, leaving the parent organic (i.e. LEV), and thus κ unchanged. No significant changes in LEV hygroscopicity were observed following exposure to O₃. This result is not surprising since O₃ is generally unreactive with aliphatic compounds and LEV is alicyclic (Seinfeld and Pandis, 1998; Knopf et al., 2011). However, as shown in Fig. 5 at higher OH exposures,
330 there is a greater separation in measured κ between purely O₃-oxidized and OH-oxidized LEV particles, indicative of the role of particle oxidation in enhancing particle hygroscopicity with increasing OH exposure.

O₃ exposure does not have a quantifiable impact on the hygroscopicity of MNC, even so MNC is aromatic and thus susceptible to O₃ addition forming a primary ozonide followed by rapid de-
335 composition to aldehydic species (Seinfeld and Pandis, 1998). This may be a result of water ad-

sorption on the surface of MNC at the RH employed, likely inhibiting O₃ uptake by MNC (Slade and Knopf, 2014; Pöschl et al., 2001; Springmann et al., 2009; Kaiser et al., 2011). The CCN activity of MNC aerosol particles increases with OH exposure as shown in the bottom panel of Fig. 5. MNC becomes more CCN active with increasing OH exposure and κ transitions from 0.009 in
 340 absence of OH to ~ 0.1 for OH exposures equivalent to a few days in the atmosphere. The data can be represented by a fit to a linear function with the form $\kappa = 10^{-13} \cdot [\text{OH}]_{\text{exp}} + 0.018$. Further exposure ($\geq 4 \cdot 10^{11}$ molecules cm⁻³ s) does not significantly enhance κ of MNC, which suggests MNC (or the particle surface (Slade and Knopf, 2014)) is fully oxidized and that the reaction products reach a maximum in κ . Similar enhancements in κ and subsequent constant κ values with increasing OH
 345 exposure have been observed for organic aerosol with initially low hygroscopicity (George et al., 2009; Lambe et al., 2011). For example, George et al. (2009) observed that κ of BES increased from ~ 0.008 to ~ 0.08 for an OH exposure of $\sim 1.5 \cdot 10^{12}$ molecule cm⁻³ s and κ of stearic acid increased from ~ 0.004 to ~ 0.04 due to OH exposure of $\sim 7.5 \cdot 10^{11}$ molecule cm⁻³ s.

The enhancement in κ of MNC following OH exposure may be linked to the formation of more
 350 hydrophilic chemical functionalities. Strongly linked to enhancements in OA hygroscopicity are larger O:C ratios (Massoli et al., 2010; Lambe et al., 2011; Mei et al., 2013a, b; Suda et al., 2014). Neglecting the oxygens in the -nitro functionality of MNC (Suda et al., 2014), the O:C ratio of pure MNC is ~ 0.29 , close to the lower end in O:C where transitions from low κ to high κ typically occurs (Suda et al., 2014). The presence of -methyl, unsaturated, and -nitro functionalities are also linked
 355 to low hygroscopicity (Suda et al., 2014). As proposed in Slade and Knopf (2014) and observed for other nitro-phenolic species, OH oxidation of MNC can favor removal of the -nitro functionality by electrophilic substitution of OH (Slade and Knopf, 2013; Di Paola et al., 2003; Chen et al., 2007). OH substitution at the -methyl position and addition to the double bonds is also possible (Anbar et al., 1966). OH addition to the -nitro or -methyl functionality would increase O:C to ~ 0.43 or
 360 ~ 0.5 , respectively. OH substitution at both positions would enhance O:C to ~ 0.67 . Suda et al. (2014) showed that hydroxyl-dominated OA with an O:C of less than ~ 0.3 has an apparent κ of $\leq 10^{-3}$. However, an increase in O:C to 0.4 or 0.6 due to the addition of hydroxyl, aldehydic, or carboxylic functionalities results in an enhanced κ of ~ 0.1 . Thus, small changes in O:C can significantly affect κ . Pure MNC is also sparingly soluble in water and thus κ is strongly dependent on its actual
 365 solubility, which can change depending on the oxidation level and the presence of other compounds having different solubility (Petters and Kreidenweis, 2008). Consequently, the conversion from low to high κ following OH oxidation is consistent with the addition of more hydrophilic functionalities and a molecular transition from sparingly soluble to sufficiently water-soluble compounds.

3.3 CCN activity of binary-component BBA surrogate-particles exposed to OH and O₃

370 Binary-component particles consisting of LEV:MNC, LEV:KS, and MNC:KS in 1:1 mass ratios were exposed to OH and O₃ and analyzed for their CCN activity as a function of OH and O₃ expo-

sure. The approach here is to determine if the presence of more than one component can influence the CCN activity of another following OH and O₃ oxidation, i.e. are the observed changes in hygroscopicity of the pure component particles following OH oxidation retained when mixed? Figure 6 shows κ as a function of OH and O₃ exposure for the different binary aerosol mixtures. The solid and dashed black lines in Fig. 6 display the modeled κ as a function of OH exposure using the volume mixing rule including and excluding MNC solubility limitations, respectively, based on the linear fits of κ as a function of OH exposure for pure LEV and MNC particles (Fig. 5). Modeled κ as a function of OH exposure excluding MNC solubility limitations (i.e. dashed lines in Fig. 6) assumes κ for MNC of the mixed particles is 0.16.

There are two important points to be made of the results from Fig. 6. (1) Hygroscopicity of the mixed particles is virtually unchanged as a function of OH exposure, i.e. while OH exposure significantly impacts MNC hygroscopicity alone, it does not significantly influence κ for the binary component particles containing MNC; and (2) κ and the trend in κ with OH exposure is significantly underpredicted assuming MNC solubility limitations are applicable in the volume mixing rule (solid lines in Fig. 6). Similar to the single-component particles, exposure to O₃ did not impact κ of the binary component particles. As discussed previously and demonstrated in Fig. 3, the presence of either KS or LEV influences the impact MNC solubility has on particle activation. We have shown that MNC exhibits no solubility limitations for the volume fractions applied here. Larger volume fractions of MNC would be expected to have a greater influence on κ following OH exposure. The organic content of BBA was shown to dominate hygroscopic growth, in particular the water soluble organic content (WSOC), which is largely levoglucosan (Dusek et al., 2011). Other studies have indicated that sparingly soluble organic compounds have limited importance in CCN activity of atmospheric aerosol (Dusek et al., 2003; Gasparini et al., 2006; Ervens et al., 2005; Andreae and Rosenfeld, 2008), although they are, besides completely insoluble organic material, the most likely class of compounds susceptible to hygroscopic changes following oxidation due to their low water-solubility. In other words, there is more room for an enhancement in the solute effect of sparingly soluble organic particles compared to more water-soluble particles. Our results show that oxidative aging impacts on the hygroscopicity of pure component particles can be vastly different if the particles are internally mixed with substances having different water-solubilities. Further highlighting this point as shown in Fig. 6, are the similar κ values measured in the absence (O₃ only) and presence of OH at the highest OH exposures for the particles containing MNC.

3.4 CCN activity of ternary-component BBA surrogate-particles exposed to OH and O₃

Here we investigate the CCN activity of internally mixed LEV, MNC, and KS particles with 1:1:1 and with an atmospherically relevant mass ratio of 1:0.03:0.3 (LEV:MNC:KS) following exposure to OH and O₃. The results are shown in Fig. 7.

Within the uncertainty of the measured κ values for the 1:1:1 and 1:0.03:0.3 ternary component particles, their hygroscopicities are virtually unaffected by exposure to OH, similar to the binary mixtures; however, on average the 1:1:1 particle mixture exhibits a slight enhancement in hygroscopicity. The predicted κ values for the 1:1:1 mixture, which include MNC solubility limitations (black line), significantly underestimates κ , and only after removing these limitations (dashed line) do the predicted values agree with measured κ . This is not surprising, given that the more water-soluble components, LEV and KS are present at equal mass to MNC, and thus MNC behaves as if it is infinitely soluble during CCN activation. At the highest OH exposures, κ in the presence of OH is on average larger than κ of the particles exposed to only O_3 , which suggests that OH oxidation may enhance the hygroscopicity of mixed BBA particles containing sparingly soluble material, albeit at large volume fractions. One possible explanation for the slight enhancement in κ with OH exposure, which differs from the binary mixed particles, is the presence of both MNC and LEV, which both exhibit enhancements in κ following OH oxidation. However, the range in measured κ at a given OH exposure is sufficiently large that within experimental uncertainty, there is no significant trend in κ with OH exposure.

The WSOC, mostly LEV, is known to dominate the volume fraction of BBA (Dusek et al., 2011). MNC constitutes $\leq 5\%$ by mass of the organic fraction of BBA as shown in both field and lab chamber studies (Iinuma et al., 2010; Claeys et al., 2012). The remaining fraction can be largely composed of inorganic salts, including KS (Pósfai et al., 2003; Rissler et al., 2006). To simulate atmospheric BBA, we atomized a mixed aqueous solution of LEV, MNC, and KS in a mass ratio of 1:0.03:0.3 and measured its CCN activity unexposed and after exposure to OH and O_3 . The resulting κ of this mixture as a function of OH and O_3 exposure is displayed in the bottom panel of Fig. 7. As anticipated, since pure LEV shows little enhancement in CCN activity with OH exposure (Fig. 5) and dominates the volume fraction of this mixture, and KS is unreactive to OH, there were no measured enhancements in κ following OH exposure. A similar observation was made from laboratory-controlled burns, whereby following several hours of photo-oxidation, there were very slight enhancements in κ of the particles (Martin et al., 2013). Larger enhancements in κ were observed only for the SOA particles generated from oxidative aging of gas phase volatiles emitted during the controlled burns, in the absence of seed particles (Martin et al., 2013). This implies that photo-oxidative aging of BBA contributes little to changes in its hygroscopicity, unless the entire aerosol population is comprised of SOA material (e.g. MNC). Furthermore, both predicted κ including solubility limitations and without solubility limitations are in agreement with the measured values. This is due to the low mass fraction of MNC present, which has sufficiently low impact on both the solubility and level of oxidation of the mixed aerosol particles.

3.5 Mixing state effects on κ

Internally mixed organic-inorganic atmospheric aerosol particles can exhibit phase separations, i.e. core-shell structure, which often contains an insoluble or solid inorganic core with a more viscous organic outer layer (Cruz and Pandis, 1998; Pósfai et al., 1998; Russell et al., 2002). The presence of an organic coating has been shown to impact CCN activity and water uptake (Cruz and Pandis, 1998; Abbatt et al., 2005; Garland et al., 2005), ice nucleation efficiency (Knopf et al., 2014; Wang et al., 2012; Baustian et al., 2012; Friedman et al., 2011; Möhler et al., 2008), and heterogeneous chemistry (Katrib et al., 2004; Gierlus et al., 2012; Knopf et al., 2007; Cosman et al., 2008). Because MNC originates from gas-phase chemical reactions, and has been measured in BBA particles, MNC must partition from the gas to the particulate phase. In this section, we investigate if the mixing state of mixed MNC and KS particles has any effect on its CCN activity following OH exposure by the application of atomized MNC:KS binary component particles and MNC-coated KS particles. For example, Abbatt et al. (2005) observed a complete deactivation in the CCN activity of ammonium sulfate particles when thickly coated with stearic acid.

The CCN activity of KS particles coated with MNC was measured as a function of the organic volume fraction ($V_{f,org}$) of MNC, and before and after OH exposure as shown in Fig. 8A. Figure 8A displays a colormap of the dry KS particle size distribution evolution following exposure to MNC, where time=0 min is the point at which KS particle growth occurred by MNC condensation. The 50th percentile of the number-weighted particle size distribution evolved from $D_p=40$ nm to $D_p=60$ nm as indicated by the black line in Fig. 8A, corresponding to an enhancement in the MNC $V_{f,org}$ from 0% at time=0 min to $\sim 70\%$ shortly after, close to the $V_{f,org}$ of the atomized MNC:KS binary component particles of 64%. The similar $V_{f,org}$ between the atomized and coated MNC/KS particles enables a direct intercomparison of the CCN activity, since relatively larger MNC $V_{f,org}$ would bias towards lower κ and vice versa.

The particles' hygroscopicity was analyzed throughout the period of condensational growth as demonstrated in Fig. 8B and shown as the black circles. The black line in Fig. 8B displays the steps in S over the course of the experiment. The first two κ values are of pure KS particles evaluated at $S=0.2\%$. Subsequent κ values are of MNC-coated KS particles, which increase in $V_{f,org}$ with time. The change in $V_{f,org}$ with time is indicated by the blue circles. $V_{f,org}$ allows to compare measured κ with that predicted using the volume mixing rule. As previously discussed, the solubility limitations of pure MNC can be neglected when predicting κ of the atomized 1:1 mass ratio MNC:KS binary component particles. To determine if the solubility of MNC impacts the MNC-coated KS particles similarly to the atomized mixture, κ is predicted using the volume mixing rule and applying a pure MNC κ of $0.009(\pm 0.005)$ (i.e. measured pure MNC κ , which includes solubility limitations) as shown by the dotted line in Fig. 8B, and compared to predicted κ applying a pure MNC κ of 0.16 (i.e. pure MNC κ in the absence of solubility limitations calculated from Eq. 6) as indicated in the dashed line in Fig. 8B. The predicted κ with increasing $V_{f,org}$ generally captures the measured trend

in κ with increasing $V_{f,org}$, however, similar to the atomized MNC:KS binary component particles, assuming MNC CCN activity is limited by its solubility, the volume mixing rule underpredicts measured κ . When applying a pure MNC $\kappa=0.16$ in the absence of solubility limitations, the volume mixing rule is in slightly better agreement with the measured κ values. However, there are notable deviations between measured κ and predicted κ in both cases, which depend on S . For example, in Fig. 8B, the predicted κ including MNC solubility limitations (dotted line) is in better agreement with the measured κ at $S=0.425\%$ than at lower S . At higher S , the particles that activate first are smaller in diameter than the particles that activate first at lower S . Assuming different sized KS particles were exposed to an equal quantity of gas-phase MNC, the larger particles, having relatively larger surface area than the smaller KS particles, would acquire a thinner organic coating, and thus relatively smaller $V_{f,org}$. As a result, the particles that activate at $S=0.425\%$ possess a larger $V_{f,org}$ compared to the particles that activate at e.g. $S=0.2\%$. This corresponds to a decrease in measured κ at $S=0.425\%$ (i.e. better agreement with predicted κ including MNC solubility limitations) relative to other S as indicated in Fig. 8B. While this experimental limitation is a source of uncertainty in the CCN activity analysis of the MNC-coated KS particles, it is included in the reported averaged κ values, since the averaged κ includes κ measured at different S . However, the generally better agreement in the predicted κ excluding MNC solubility limitations with the measured κ indicates that MNC is sufficiently water-soluble not deactivating KS, in contrast to the particle systems studied by Abbatt et al. (2005).

The effects of OH exposure on the CCN activity of MNC-coated KS particles as a function of $V_{f,org}$ is given in Fig. 8C. κ is plotted as a function of MNC $V_{f,org}$. The κ values resulting from an OH exposure of 3.3×10^{11} molecule cm^{-3} s are given by the black circles. Gray circles correspond to κ in the absence of OH. At $V_{f,org}=0\%$ κ is ~ 0.55 and independent of OH exposure. κ decreases to ~ 0.24 at $V_{f,org} \approx 70\%$, but undergoes a slight enhancement to ~ 0.3 following exposure to OH. The dotted gray line indicates the modeled change in unexposed κ as a function of $V_{f,org}$ applying the volume mixing rule and assuming MNC $\kappa=0.009$ (i.e. including MNC solubility limitations). The modeled κ slightly underpredicts measured κ , which suggests in the presence of KS at this $V_{f,org} \approx 70\%$, MNC may not be limited by its solubility, similar to the atomized 1:1 mass ratio MNC:KS binary component particles. However, the dashed gray line shows the modeled κ as a function of $V_{f,org}$ applying the volume mixing rule and assuming MNC is not limited by its solubility, i.e. MNC $\kappa=0.16$, which slightly over predicts the measured κ . A reasonable explanation for this is that $V_{f,org} \approx 70\%$ is sufficiently large such that MNC solubility limitations on the CCN activity of MNC-coated KS particles are partially exhibited. The dashed black line in Fig. 8C shows the modeled change in κ as a function of $V_{f,org}$ for the OH exposed particles excluding MNC solubility limitations and applying the volume mixing rule assuming κ of MNC has adjusted to the applied OH exposure based on the linear fit to κ of MNC as a function of OH exposure (Fig. 5). The modeled κ is in good agreement with the measured κ for the OH exposed particles, which suggests it is reasonable

515 to assume MNC is not significantly limited by its solubility at $V_{f,org} \approx 70\%$ for the MNC-coated KS particles. While OH exposure has a significant impact on the CCN activity of pure MNC, its impact on the CCN activity of MNC-coated KS particles is significantly less, and the higher water-solubility of KS governs hygroscopic growth, similar to the atomized MNC:KS binary component particles.

4 Conclusions

520 To our knowledge, there are no studies that have explicitly investigated the influence of OH-initiated oxidative aging on the hygroscopicity of organic and mixed organic-inorganic BBA particles. Biomass burning can greatly influence cloud formation and microphysical properties by increasing the available CCN in the atmosphere (Andreae et al., 2004). However, the efficiency at which aerosol particles act as CCN depends on their water solubility, hygroscopicity, and size, which can be altered by
525 multiphase chemical reactions with gas-phase oxidants. While it is recognized that a significant fraction of BBA are comprised of organic material (Reid et al., 2005), most of which are water-soluble (Dusek et al., 2011; Graham et al., 2002), water uptake can be sensitive to the inorganic mass fraction (Semeniuk et al., 2007; Ruehl et al., 2012). In this study we investigated how sensitive the CCN activity of single-component and mixed water-soluble/insoluble compounds associated with BBA
530 are to OH oxidation. The important findings relevant to the atmosphere include (i) the hygroscopicity of water-soluble organic compounds is unaffected by chemical aging, (ii) The hygroscopicity of single-component water-insoluble organic compounds is affected by chemical aging as anticipated from previous studies (George et al., 2009; Lambe et al., 2011; Wong et al., 2011; Broekhuizen et al., 2004; Shilling et al., 2007; Petters et al., 2006), and (iii) if considering mixtures of water-soluble and
535 insoluble materials, the effects of chemical aging by OH are more complicated and single-component derived κ and changes to κ as a function of OH exposure do not translate directly to mixtures.

WSOC constitutes a significant fraction of biomass burning OA (Graham et al., 2002; Reid et al., 2005; Saarikoski et al., 2007; Saarnio et al., 2010; Dusek et al., 2011) and atmospheric OA in general (Saxena and Hildemann, 1996; Timonen et al., 2013). Water-soluble OA is an effective CCN because
540 it enhances the solute term in the Köhler equation. Chemical aging is known to promote the solubility of initially insoluble and sparingly soluble OA by yielding more water-soluble and multifunctional reaction products (George et al., 2009; Petters et al., 2006; Decesari et al., 2002). The question of atmospheric relevance depends on the concentration or potency of a particular molecule in the atmosphere. MNC, while contributing little to the mass fraction of BBA particles, is toxic to forests
545 (Harrison et al., 2005) and recognized as an important biomass burning SOA molecular marker (Iinuma et al., 2010). An OH exposure equivalent to only a few days of atmospheric exposure leads to an order of magnitude enhancement in MNC hygroscopicity. This implies that aged MNC is more susceptible to wet depositional losses over atmospherically relevant particle transport timescales, e.g. through cloud formation, compared to fresh MNC. Calculations from Petters et al. (2006) indicate

that substantial wet depositional losses can occur when $\kappa > 0.01$. The question of the utility of MNC as a molecular marker for source apportionment is raised since molecular markers are assumed to be inert over the course of its lifetime in the atmosphere. Clearly, OH oxidation of MNC influences its chemical composition, but in doing so also decreases its atmospheric lifetime by enhancing its CCN activity. However, our results strongly suggest if the OA is WSOC-dominated, e.g. by LEV, the reaction products likely have similar CCN activity to the parent WSOC, and thus particle oxidation plays a very minor role in enhancing the CCN activity of WSOC. Indeed, very little enhancements to the hygroscopicity of BBA produced from controlled wood burning resulted from several hours of photo-oxidation, likely a result of the high WSOC content of BBA (Martin et al., 2013).

Much less is known of the effects of chemical aging on the CCN activity of internally mixed water-soluble and insoluble organic-inorganic particles. While oxidative aging can enhance the hygroscopicity of single-component particles with initially low water-solubility, atmospheric aerosol particles are not often pure and consist of both organic and inorganic compounds (Laskin et al., 2012; Knopf et al., 2014; Murphy and Thomson, 1997; Murphy et al., 2006; Middlebrook et al., 1998). Organic compounds alone can influence the hygroscopicity of inorganic aerosol particles (Marcolli et al., 2004; Choi and Chan, 2002; Svenningsson et al., 2006; Wang et al., 2008) and moderate amounts of water-soluble inorganics can render low-solubility organics infinitely water-soluble (Bilde and Svenningsson, 2004; Abbatt et al., 2005; Shantz et al., 2008; Petters and Kreidenweis, 2008). When mixed with LEV or KS (or both) in significant mass fractions, the effects of OH oxidative aging on the hygroscopicity of single-component MNC are not revealed in the measured κ for the binary or ternary-component particles. Furthermore, a thick coating of MNC on KS particles had similar impacts on the CCN activity behavior with increasing OH exposure as the atomized binary-component MNC:KS particles. The water-soluble fraction (i.e. KS) was sufficiently large that MNC became infinitely soluble. Our results indicate that it is the fraction of the water-soluble component of internally mixed water-soluble and insoluble organic-inorganic particles that dictates whether chemical aging will enhance the particles' CCN activity. Chemical aging has no major impact on the CCN activity of mixed water-soluble and insoluble compounds beyond the point that the insoluble component becomes infinitely soluble. Below this point, chemical aging can influence the CCN activity of the insoluble component.

Acknowledgements. J.H. Slade and D.A. Knopf acknowledge support from the National Science Foundation grants OCE-1336724 and AGS-0846255. J. Wang and R. Thalman acknowledge support from the U.S. Department of Energy's Atmospheric System Research Program (Office of Science, OBER) under contract DE-AC02098CH10886.

References

References

- Abbatt, J. P. D., Broekhuizen, K., and Kumal, P. P.: Cloud condensation nucleus activity of internally mixed ammonium sulfate/organic acid aerosol particles, *Atmos. Environ.*, 39, 4767–4778, doi:10.1016/j.atmosenv.2005.04.029, 2005.
- Abbatt, J. P. D., Lee, A. K. Y., and Thornton, J. A.: Quantifying trace gas uptake to tropospheric aerosol: recent advances and remaining challenges, *Chem. Soc. Rev.*, 41, 6555–6581, doi:10.1039/c2cs35052a, 2012.
- Anbar, M., Meyerstein, D., and Neta, P.: The reactivity of aromatic compounds toward hydroxyl radicals, *J. Phys. Chem.*, 70, 2660–2662, doi:10.1021/j100880a034, 1966.
- Andreae, M. O. and Rosenfeld, D.: Aerosol-cloud-precipitation interactions. Part 1. The nature and sources of cloud-active aerosols, *Earth-Sci. Rev.*, 89, 13–41, doi:10.1016/j.earscirev.2008.03.001, 2008.
- Andreae, M. O., Rosenfeld, D., Artaxo, P., Costa, A. A., Frank, G. P., Longo, K. M., and Silva-Dias, M. A. F.: Smoking rain clouds over the Amazon, *Science*, 303, 1337–1342, doi:10.1126/science.1092779, 2004.
- Arangio, A., Slade, J. H., Berkemeier, T., Pöschl, U., Knopf, D. A., and Shiraiwa, M.: Multiphase chemical kinetics of OH radical uptake by molecular organic markers of biomass burning aerosols: humidity and temperature dependence, surface reaction and bulk diffusion, *J. Phys. Chem. A.*, 2014.
- Bai, J., Sun, X., Zhang, C., Xu, Y., and Qi, C.: The OH-initiated atmospheric reaction mechanism and kinetics for levoglucosan emitted in biomass burning, *Chemosphere*, 93, 2004–2010, doi:10.1016/j.chemosphere.2013.07.021, 2013.
- Baustian, K. J., Cziczo, D. J., Wise, M. E., Pratt, K. A., Kulkarni, G., Hallar, A. G., and Tolbert, M. A.: Importance of aerosol composition, mixing state, and morphology for heterogeneous ice nucleation: A combined field and laboratory approach, *J. Geophys. Res.-Atmos.*, 117, D06 217, doi:10.1029/2011JD016784, 2012.
- Bilde, M. and Svenningsson, B.: CCN activation of slightly soluble organics: the importance of small amounts of inorganic salt and particle phase, *Tellus*, 56B, 128–134, doi:10.1111/j.1600-0889.2004.00090.x, 2004.
- Bond, T., Streets, D., Yarber, K., Nelson, S., Woo, J.-H., and Klimont, Z.: A technology-based global inventory of black and organic carbon emissions from combustion, *J. Geophys. Res.*, 109, D14 203, doi:10.1029/2003JD003697, 2004.
- Broekhuizen, K. E., Thornberry, T., Kumar, P. P., and Abbatt, J. P. D.: Formation of cloud condensation nuclei by oxidative processing: Unsaturated fatty acids, *J. Geophys. Res.*, 109, S524–S537, doi:10.1029/2004JD005298, 2004.
- Brooks, S. D., Suter, K., and Olivarez, L.: Effects of chemical aging on the ice nucleation activity of soot and polycyclic aromatic hydrocarbon aerosols, *J. Phys. Chem. A.*, 118, 10036–10047, doi:10.1021/jp508809y, 2014.
- Carrico, C. M., Petters, M. D., Kreidenweis, S. M., Sullivan, A. P., McMeeking, G. R., Levin, E. J. T., Engling, G., Malm, W. C., and Collett Jr., J. L.: Water uptake and chemical composition of fresh aerosols generated in open burning of biomass, *Atmos. Chem. Phys.*, 10, 5165–5178, doi:10.5194/acp-10-5165-2010, 2010.

- Chan, M. N., Choi, M. Y., Ng, N. L., and Chan, C. K.: Hygroscopicity of water-soluble organic compounds in atmospheric aerosols: Amino acids and biomass burning derived organic species, *Environ. Sci. Technol.*, 39, 1555–1562, doi:10.1021/es049584I, 2005.
- 625 Chen, L., Moosmuller, H., Arnott, W., Chow, J., Watson, J., Susott, R., Babbitt, R., Wold, C., Lincoln, E., Hao, W., Moosmuller, H., Arnott, W. P., Chow, J. C., Watson, J. G., Susott, R. A., Babbitt, R. E., Wold, C. E., Lincoln, E. N., and Hao, W. M.: Emissions from laboratory combustion of wildland fuels: Emission factors and source profiles, *Environ. Sci. Technol.*, 41, 4317–4325, doi:10.1021/es062364i, 2007.
- Choi, M. Y. and Chan, C. K.: The effects of organic species on the hygroscopic behaviors of inorganic aerosols, *Environ. Sci. Technol.*, 36, 2422–2428, doi:10.1021/es0113293, 2002.
- 630 Claey's, M., Vermeylen, R., Yasmeen, F., Gómez-González, Y., Chi, X., Maenhaut, W., Mészáros, T., and Salma, I.: Chemical characterisation of humic-like substances from urban, rural and tropical biomass burning environments using liquid chromatography with UV/vis photodiode array detection and electrospray ionisation mass spectrometry, *Environ. Chem.*, 9, 273–284, doi:10.1071/EN11163, 2012.
- 635 Collins, D. R., Flagan, R. C., and Seinfeld, J. H.: Improved inversion of scanning DMA data, *Aerosol Sci. Technol.*, 36, 1–9, doi:10.1080/027868202753339032, 2002.
- Cosman, L. M., Knopf, D. A., and Bertram, A. K.: N_2O_5 reactive uptake on aqueous sulfuric acid solutions coated with branched and straight-chain insoluble organic surfactants, *J. Phys. Chem. A.*, 112, 2386–2396, doi:10.1021/jp710685r, 2008.
- 640 Cruz, C. N. and Pandis, S. N.: The effect of organic coatings on the cloud condensation nuclei activation of inorganic atmospheric aerosol, *J. Geophys. Res.-Atmos.*, 103, 13 111–13 123, doi:10.1029/98JD00979, 1998.
- Decesari, S., Facchini, M. C., Matta, E., Mircea, M., Fuzzi, S., Chughtai, A. R., and Smith, D. M.: Water soluble organic compounds formed by oxidation of soot, *Atmos. Environ.*, 36, 1827–1832, doi:10.1016/S1352-2310(02)00141-3, 2002.
- 645 Di Paola, A., Augugliaro, V., Palmisano, L., Pantaleo, G., and Savinov, E.: Heterogeneous photocatalytic degradation of nitrophenols, *J. Photoch. Photobio. A*, 155, 207–214, doi:10.1016/S1010-6030(02)00390-8, 2003.
- Dusek, U., Covert, D. S., Wiedensohler, A., Neususs, C., Weise, D., and Cantrell, W.: Cloud condensation nuclei spectra derived from size distributions and hygroscopic properties of the aerosol in coastal southwest Portugal during ACE-2, *Tellus B.*, 55, 35–53, doi:10.1034/j.1600-0889.2002.00041.x, 2003.
- 650 Dusek, U., Frank, G. P., Hildebrandt, L., Curtius, J., Schneider, J., Walter, S., Chand, D., Drewnick, F., Hings, S., Jung, D., Borrmann, S., and Andreae, M. O.: Size matters more than chemistry for cloud-nucleating ability of aerosol particles, *Science*, 312, 1375–1378, doi:10.1126/science.1125261, 2006.
- 655 Dusek, U., Frank, G. P., Massling, A., Zeromskiene, K., Iinuma, Y., Schmid, O., Helas, G., Hennig, T., Wiedensohler, A., and Andreae, M. O.: Water uptake by biomass burning aerosol at sub- and supersaturated conditions: closure studies and implications for the role of organics, *Atmos. Chem. Phys.*, 11, 9519–9532, doi:10.5194/acp-11-9519-2011, 2011.
- Ellison, G. B., Tuck, A. F., and Vaida, V.: Atmospheric processing of organic aerosols, *J. Geophys. Res.-Atmos.*, 104, 11 633–11 641, doi:10.1029/1999JD900073, 1999.
- 660

Ervens, B., Feingold, G., and Kreidenweis, S. M.: Influence of water-soluble organic carbon on cloud drop number concentration, *J. Geophys. Res.-Atmos.*, 110, D18 211, doi:10.1029/2004JD005634, 2005.

Friedman, B., Kulkarni, G., Beránek, J., Zelenyuk, A., Thornton, J. A., and Cziczo, D. J.: Ice nucleation and droplet formation by bare and coated soot particles, *J. Geophys. Res.*, 116, D17 203, doi:10.1029/2011JD015999, 2011.

Fuchs, N. A. and Sutugin, A. G.: Highly Dispersed Aerosols, *Ann Arbor Sci.*, 2nd edn., 1970.

Garland, R. M., Wise, M. E., Beaver, M. R., DeWitt, H. L., Aiken, A. C., Jimenez, J. L., and Tolbert, M. A.: Impact of palmitic acid coating on the water uptake and loss of ammonium sulfate particles, *Atmos. Chem. Phys.*, 5, 1951–1961, doi:10.5194/acp-5-1951-2005, 2005.

Gasparini, R., Li, R. J., Collins, D. R., Ferrare, R. A., and Brackett, V. G.: Application of aerosol hygroscopicity measured at the Atmospheric Radiation Measurement Program’s Southern Great Plains site to examine composition and evolution, *J. Geophys. Res.-Atmos.*, 111, D05S12, doi:10.1029/2004JD005448, 2006.

George, I. J. and Abbatt, J. P. D.: Heterogeneous oxidation of atmospheric aerosol particles by gas-phase radicals, *Nat. Chem.*, 2, 713–722, doi:10.1038/nchem.806, 2010.

George, I. J., Chang, R. Y.-W., Danov, V., Vlasenko, A., and Abbatt, J. P. D.: Modification of cloud condensation nucleus activity of organic aerosols by hydroxyl radical heterogeneous oxidation, *Atmos. Environ.*, 43, 5038–5045, doi:10.1016/j.atmosenv.2009.06.043, 2009.

Gierlus, K. M., Laskina, O., Abernathy, T. L., and Grassian, V. H.: Laboratory study of the effect of oxalic acid on the cloud condensation nuclei activity of mineral dust aerosol, *Atmos. Environ.*, 46, 125–130, doi:10.1016/j.atmosenv.2011.10.027, 2012.

Giordano, M., Espinoza, C., and Asa-Awuku, A.: Experimentally measured morphology of biomass burning aerosol and its impacts on CCN ability, *Atmos. Chem. Phys. Discuss.*, 14, 12 555–12 589, doi:10.5194/acpd-14-12555-2014, 2014.

Graham, B., Mayol-Bracero, O. L., Guyon, P., Roberts, G. C., Decesari, S., Facchini, M. C., Artaxo, P., Maenhaut, W., Koll, P., and Andreae, M. O.: Water-soluble organic compounds in biomass burning aerosols over Amazonia - 1. Characterization by NMR and GC-MS, *J. Geophys. Res.-Atmos.*, 107, 8047, doi:10.1029/2001JD000336, 2002.

Grieshop, A. P., Logue, J. M., Donahue, N. M., and Robinson, A. L.: Laboratory investigation of photochemical oxidation of organic aerosol from wood fires 1: measurement and simulation of organic aerosol evolution, *Atmos. Chem. Phys.*, 9, 1263–11 277, doi:10.5194/acp-9-2227-2009, 2009.

Gunthe, S. S., King, S. M., Rose, D., Chen, Q., Roldin, P., Farmer, D. K., Jimenez, J. L., Artaxo, P., Andreae, M. O., Martin, S. T., and Pöschl, U.: Cloud condensation nuclei in pristine tropical rainforest air of Amazonia: size-resolved measurements and modeling of atmospheric aerosol composition and CCN activity, *Atmos. Chem. Phys.*, 9, 7551–7575, doi:10.5194/acp-9-7551-2009, 2009.

Hallquist, M., Wenger, J. C., Baltensperger, U., Rudich, Y., Simpson, D., Claeys, M., Dommen, J., Donahue, N. M., George, C., Goldstein, A. H., Hamilton, J. F., Herrmann, H., Hoffmann, T., Iinuma, Y., Jang, M., Jenkin, M. E., Jimenes, J. L., Kiendler-Scharr, A., Maenhaut, W., McFiggans, G., Mentel, T. F., Monod, A., Prévôt, A. S. H., Seinfeld, J. H., Surratt, J. D., Szmigielski, R., and Wildt, J.: The formation, properties

700 and impact of secondary organic aerosol: current and emerging issues, *Atmos. Chem. Phys.*, 9, 5155–5236, doi:10.5194/acp-9-5155-2009, 2009.

Harmon, C. W., Ruehl, C. R., Cappa, C. D., and Wilson, K. R.: A statistical description of the evolution of cloud condensation nuclei activity during the heterogeneous oxidation of squalane and bis(2-ethylhexyl) sebacate aerosol by hydroxyl radicals, *Phys. Chem. Chem. Phys.*, 15, 9679–9693, doi:10.1039/C3CP50347J, 2013.

705 Harrison, M. A. J., Barra, S., Borghesi, D., Vione, D., Arsene, C., and Olariu, R. I.: Nitrated phenols in the atmosphere: a review, *Atmos. Environ.*, 39, 231–248, doi:10.1016/j.atmosenv.2004.09.044, 2005.

Hays, M. D., Fine, P. M., Geron, C. D., Kleeman, M. J., and Gullett, B. K.: Open burning of agricultural biomass: Physical and chemical properties of particle-phase emissions, *Atmos. Environ.*, 39, 6747–6764, doi:10.1016/j.atmosenv.2005.07.072, 2005.

710 Hoffmann, D., Tilgner, A., Iinuma, Y., and Herrmann, H.: Atmospheric stability of levoglucosan: a detailed laboratory and modeling study, *Environ. Sci. Technol.*, 44, 694–699, doi:10.1021/es902476f, 2010.

Iinuma, Y., Brüggemann, E., Gnauk, T., Müller, K., Andreae, M., Helas, G., Parmar, R., and Herrmann, H.: Source characterization of biomass burning particles: the combustion of selected European conifers, African hardwood, savanna grass, and German and Indonesian peat, *J. Geophys. Res.*, 112, D08 209, doi:10.1029/2006JD007120, 2007.

715 Iinuma, Y., Bøge, O., Gräfe, R., and Herrmann, H.: Methyl-nitrocatechols: atmospheric tracer compounds for biomass burning secondary organic aerosols, *Environ. Sci. Technol.*, 44, 8453–8459, doi:10.1021/es102938e, 2010.

720 Jathar, S. H., Gordon, T. D., Hennigan, C. J., Pye, H. O. T., Pouliot, G., Adams, P. J., Donahue, N. M., and Robinson, A. L.: Unspeciated organic emissions from combustion sources and their influence on the secondary organic aerosol budget in the United States, *Proc. Nat. Acad. Sci.*, 111, 10 473–10 478, doi:10.1073/pnas.1323740111, 2014.

Kaiser, C., Riemer, N., and Knopf, D. A.: Detailed heterogeneous oxidation of soot surfaces in a particle-resolved aerosol model, *Atmos. Chem. Phys.*, 11, 4505–4520, doi:10.5194/acp-11-4504-2011, 2011.

725 Katrib, Y., Martin, S. T., Hung, H. M., Rudich, Y., Zhang, H. Z., Slowik, J. G., Davidovits, P., Jayne, J. T., and Worsnop, D. R.: Products and mechanisms of ozone reactions with oleic acid for aerosol particles having core-shell morphologies, *J. Phys. Chem. A*, 108, 6686–6695, doi:10.1021/jp049759d, 2004.

Kessler, S. H., Smith, J. D., Che, D. L., Worsnop, D. R., Wilson, K. R., and Kroll, J. H.: Chemical sinks of organic aerosol: kinetics and products of the heterogeneous oxidation of erythritol and levoglucosan, *Environ. Sci. Technol.*, 44, 7005–7010, doi:10.1021/es101465m, 2010.

730 Knopf, D. A., Cosman, L. M., Mousavi, P., Mokamati, S., and Bertram, A. K.: A Novel Flow Reactor for Studying Reactions on Liquid Surfaces Coated by Organic Monolayers: Methods, Validation, and Initial Results, *J. Phys. Chem. A*, 111, 11 021–11 032, 2007.

735 Knopf, D. A., Forrester, S. M., and Slade, J. H.: Heterogeneous oxidation kinetics of organic biomass burning aerosol surrogates by O₃, NO₂, N₂O₅, and NO₃, *Phys. Chem. Chem. Phys.*, 13, 21 050–21 062, doi:10.1039/c1cp22478f, 2011.

- Knopf, D. A., Alpert, P. A., Wang, B., O'Brien, E., Kelly, S. T., Laskin, A., Gilles, K., and Moffet, R. C.: Microspectroscopic imaging and characterization of individually identified ice nucleating particles from a case field study, *J. Geophys. Res.*, 119, 10 365–10 381, doi:10.1002/2014JD021866, 2014.
- Lambe, A. T., Onasch, T. B., Massoli, P., Croasdale, D. R., Wright, J. P., Ahern, A. T., Williams, L. R., Worsnop, D. R., Brune, W. H., and Davidovits, P.: Laboratory studies of the chemical composition and cloud condensation nuclei activity of secondary organic aerosol and oxidized primary organic aerosol, *Atmos. Chem. Phys.*, 11, 8913–8928, doi:10.5194/acp-11-8913-2011, 2011.
- Lance, S., Medina, J., Smith, J. N., and Nenes, A.: Mapping the operation of the DMT Continuous Flow CCN counter, *Aerosol Sci. Technol.*, 40, 242–254, doi:10.1080/02786820500543290, 2006.
- Laskin, A., Moffet, R. C., Gilles, M. K., Fast, J. D., Zaveri, R. A., Wang, B., Nigge, P., and Shutthanandan, J.: Tropospheric chemistry of internally mixed sea salt and organic particles: Surprising reactivity of NaCl with weak organic acids, *J. Geophys. Res.*, 117, doi:10.1029/2012JD017743, 2012.
- Low, R. D. H.: A comprehensive report on nineteen condensation nuclei. Part 1. Equilibrium growth and physical properties, Army Electronics Command, White Sands Missile Range, NM Atmospheric Sciences Lab, 1969.
- Marcolli, C., Luo, B. P., and Peter, T.: Mixing of the organic aerosol fractions: Liquids as the thermodynamically stable phases, *J. Phys. Chem. A*, 108, 2216–2224, doi:10.1021/jp036080I, 2004.
- Martin, M., Tritscher, T., Jurányi, Z., Heringa, M. F., Sierau, B., Weingartner, E., Chirico, R., Gysel, M., Preévôt, A. S. H., Baltensperger, U., and Lohmann, U.: Hygroscopic properties of fresh and aged wood burning particles, *J. Aerosol. Sci.*, 56, 15–29, doi:10.1016/j.jaerosci.2012.08.006, 2013.
- Massoli, P., Lambe, A. T., Ahern, A. T., Williams, L. R., Ehn, M., Mikkilä, J., Canagaratna, M. R., Brune, W. H., Onasch, T. B., Jayne, J. T., Petäjä, T., Kulmala, M., Laaksonen, A., Kolb, C. E., Davidovits, P., and Worsnop, D. R.: Relationship between aerosol oxidation level and hygroscopic properties of laboratory generated secondary organic aerosol (SOA) particles, *Geophys. Res. Lett.*, 37, L24 801, doi:10.1029/2010GL045258, 2010.
- Mei, F., Hayes, P. L., Ortega, A., Taylor, J. W., Allan, J. D., Gilman, J., Kuster, W., de Gouw, J., Jimenez, J. L., and Wang, J.: Droplet activation properties of organic aerosols observed at an urban site during CalNex-LA, *J. Geophys. Res.-Atmos.*, 118, 2903–2917, doi:10.1002/jgrd.50285, 2013a.
- Mei, F., Setyan, A., Zhang, Q., and Wang, J.: CCN activity of organic aerosols observed downwind of urban emissions during CARES, *Atmos. Chem. Phys.*, 13, 12 155–12 169, doi:10.5194/acp-13-12155-2013, 2013b.
- Middlebrook, A. M., Murphy, D. M., and Thomson, D. S.: Observations of organic material in individual marine particles at Cape Grim during the First Aerosol Characterization Experiment (ACE 1), *J. Geophys. Res.*, 103, 16 475–16 483, doi:10.1029/97JD03719, 1998.
- Mikhailov, E., Vlasenko, S., Martin, S. T., Koop, T., and Pöschl, U.: Amorphous and crystalline aerosol particles interacting with water vapor: conceptual framework and experimental evidence for restructuring, phase transitions and kinetic limitations, *Atmos. Chem. Phys.*, 9, 9491–9522, doi:10.5194/acp-9-9491-2009, 2009.

Möhler, O., Benz, S., Saathoff, H., Schnaiter, M., Wagner, R., Schneider, J., Walter, S., Ebert, V., and Wagner, S.: The effect of organic coating on the heterogeneous ice nucleation efficiency of mineral dust aerosols, *Environ. Res. Lett.*, 3, 10.1088/1748-9326/3/2/025007, 2008.

780 Monks, P. S., Granier, C., Fuzzi, S., Stohl, A., Williams, M. L., Akimoto, H., Amann, M., Baklanov, A., Baltensperger, U., Bey, I., Blake, N., Blake, R. S., Carslaw, K., Cooper, O. R., Dentener, F., Fowler, D., Fragkou, E., Frost, G. J., Generoso, S., Ginoux, P., Grewe, V., Guenther, A., Hansson, H. C., Henne, S., Hjorth, J., Hofzumahaus, A., Huntrieser, H., Isaksen, I. S. A., Jenkin, M. E., Kaiser, J., Kanakidou, M., Klimont, Z., Kulmala, M., Laj, P., Lawrence, M. G., Lee, J. D., Liousse, C., Maione, M., McFiggans, G., Metzger, A., Mieville, A., Moussiopoulos, N., Orlando, J. J., O'Dowd, C. D., Palmer, P. I., Parrish, D. D.,

785 Petzold, A., Platt, U., Pöschl, U., Prévôt, A. S. H., Reeves, C. E., Reimann, S., Rudich, Y., Sellegri, K., Steinbrecher, R., Simpson, D., ten Brink, H., Theloke, J., van der Werf, G. R., Vautard, R., Vestreng, V., Vlachokostas, C., and von Glasow, R.: Atmospheric composition change - global and regional air quality, *Atmos. Environ.*, 43, 5268–5350, doi:10.1016/j.atmosenv.2009.08.021, 2009.

790 Murphy, D. M. and Thomson, D. S.: Chemical composition of single aerosol particles at Idaho Hill: Negative ion measurements, *J. Geophys. Res.-Atmos.*, 102, 6353–6368, doi:10.1029/96JD00859, 1997.

Murphy, D. M., Cziczó, D. J., Froyd, K. D., Hudson, P. K., Matthew, B. M., Middlebrook, A. M., Peltier, R. E., Sullivan, A., Thomson, D. S., and Weber, R. J.: Single-particle mass spectrometry of tropospheric aerosol particles, *J. Geophys. Res.*, 111, D23S32, doi:10.1029/2006JD007340, 2006.

795 Novakov, T. and Corrigan, C. E.: Cloud condensation nucleus activity of the organic component of biomass smoke particles, *Geophys. Res. Lett.*, 23, 2141–2144, doi:10.1029/96GL01971, 1996.

Park, S.-C., Burden, D. K., and Nathanson, G. M.: The Inhibition of N₂O₅ Hydrolysis in Sulfuric Acid by 1-Butanol and 1-Hexanol Surfactant Coatings, *J. Phys. Chem. A*, 111, 2921–2929, doi:10.1021/jp068228h, 2007.

800 Petters, M. D. and Kreidenweis, S. M.: A single parameter representation of hygroscopic growth and cloud condensation nucleus activity, *Atmos. Chem. Phys.*, 7, 1961–1971, doi:10.5194/acp-7-1961-2007, 2007.

Petters, M. D. and Kreidenweis, S. M.: A single parameter representation of hygroscopic growth and cloud condensation nucleus activity - Part 2: Including solubility, *Atmos. Chem. Phys.*, 8, 6273–6279, doi:10.5194/acp-8-6273-2008, 2008.

805 Petters, M. D., Prenne, A. J., and Kreidenweis, S. M.: Chemical aging and the hydrophobic-to-hydrophilic conversion of carbonaceous aerosol, *Geophys. Res. Lett.*, 33, doi:10.1029/2006GL027249, 2006.

Petters, M. D., Carrico, C. M., Kreidenweis, S. M., Prenni, A. J., DeMott, P. J., Collett Jr., J. L., and Moosmüller, H.: Cloud condensation nucleation activity of biomass burning aerosol, *J. Geophys. Res.*, 114, D22 205, doi:10.1029/2009JD012353, 2009.

810 Pöschl, U.: Atmospheric aerosols: composition, transformation, climate and health effects, *Angew. Chem. Int. Ed.*, 44, 7520–7540, doi:10.1002/anie.200501122, 2005.

Pöschl, U.: Gas-particle interactions of tropospheric aerosols: kinetic and thermodynamic perspectives of multiphase chemical reactions, amorphous organic substances, and the activation of cloud condensation nuclei, *Atmos. Res.*, 101, 562–573, doi:10.1016/j.atmosres.2010.12.018, 2011.

815 Pöschl, U., Letzel, T., Schauer, C., and Niessner, R.: Interaction of ozone and water vapor with spark discharge soot aerosol particles coated with benzo[a]pyrene: O₃ and H₂O adsorption, benzo[a]pyrene degradation, and atmospheric implications, *J. Phys. Chem. A*, 105, 4029–4041, doi:10.1021/jp004137n, 2001.

Pósfai, M., Xu, H. F., Anderson, J. R., and Buseck, P. R.: Wet and dry sizes of atmospheric aerosol particles: an AFM-TFM study, *Geophys. Res. Lett.*, 25, 1907–1910, doi:10.1029/98GL01416, 1998.

820 Pósfai, M., Simonics, R., Li, J., Hobbs, P. V., and Buseck, P. R.: Individual aerosol particles from biomass burning in southern Africa: 1. Compositions and size distributions of carbonaceous particles, *J. Geophys. Res.-Atmos.*, 108, 231–240, doi:10.1029/2002JD002291, 2003.

Randerson, J. T., Chen, Y., van der Werf, G. R., Rogers, B. M., and Morton, D. C.: Global burned area and biomass burning emissions from small fires, *J. Geophys. Res.-Biogeo.*, 117, G04012, doi:10.1029/2012JG002128, 2012.

825 Reid, J. S., Eck, T. F., Christopher, S. A., Koppmann, R., Dubovik, O., Eleuterio, D. P., Holben, B. N., Reid, E. A., and Zhang, J.: A review of biomass burning emissions part III: intensive optical properties of biomass burning particles, *Atmos. Chem. Phys.*, 5, 827–849, doi:10.5194/acp-5-827-2005, 2005.

Renbaum, L. H. and Smith, G. D.: Artifacts in measuring aerosol uptake kinetics: the roles of time, concentration and adsorption, *Atmos. Chem. Phys.*, 11, 6881–6893, doi:10.5194/acp-11-6881-2011, 2011.

830 Rissler, J., Vestin, A., Swietlicki, E., Fisch, G., Zhou, J., Artaxo, P., and Andreae, M. O.: Size distribution and hygroscopic properties of aerosol particles from dry-season biomass burning in Amazonia, *Atmos. Chem. Phys.*, 6, 471–491, doi:10.5194/acp-6-471-2006, 2006.

Roberts, G., Artaxo, P., Zhou, J., Swietlicki, E., and Andreae, M. O.: Sensitivity of CCN spectra on chemical and physical properties of aerosol: A case study from the Amazon Basin, *J. Geophys. Res.*, 107, 8070, doi:10.1029/2001JD000583, 2002.

835 Roberts, G. C. and Nenes, A.: A continuous-flow streamwise thermal-gradient CCN chamber for atmospheric measurements, *Aerosol Sci. Technol.*, 39, 206–221, doi:10.1080/027868290913988, 2005.

Rose, D., Gunthe, S. S., Mikhailov, E., Frank, G. P., Dusek, U., Andreae, M. O., and Pöschl, U.: Calibration and measurement uncertainties of a continuous-flow cloud condensation nuclei counter (DMT-CCNC): CCN activation of ammonium sulfate and sodium chloride aerosol particles in theory and experiments,

840 *Atmos. Chem. Phys.*, 8, 1153–1179, doi:10.5194/acp-8-1153-2008, 2008.

Rose, D., Nowak, A., Achtert, P., Wiedensohler, A., Hu, M., Shao, M., Zhang, Y., Andreae, M. O., and Pöschl, U.: Cloud condensation nuclei in polluted air and biomass burning smoke near the mega-city Guangzhou, China - Part 1: Size-resolved measurements and implications for the modeling of aerosol

845 particle hygroscopicity and CCN activity, *Atmos. Chem. Phys.*, 10, 3365–3383, doi:10.5194/acp-10-3365-2010, 2010.

Rudich, Y.: Laboratory perspectives on the chemical transformations of organic matter in atmospheric particles, *Chem. Rev.*, 103, 5097–5124, doi:10.1021/cr020508f, 2003.

850 Rudich, Y., Donahue, N. M., and Mentel, T. F.: Aging of organic aerosol: bridging the gap between laboratory and field studies, *Ann. Rev. Phys. Chem.*, 58, 321–352, doi:10.1146/annurev.physchem.58.032806.104432, 2007.

Ruehl, C. R., Chuang, P. Y., Nenes, A., Cappa, C. D., Kolesar, K. R., and Goldstein, A. H.: Strong evidence of surface tension reduction in microscopic aqueous droplets, *Geophys. Res. Lett.*, 39, L23 801, doi:10.1029/2012GL053706, 2012.

855 Russell, L. M., Maria, S. F., and Myneni, S. C. B.: Mapping organic coatings on atmospheric particles, *Geophys. Res. Lett.*, 29, 26–1–26–4, doi:10.1029/2002GL014874, 2002.

Saarikoski, S., Sillanpaa, M., Sofiev, M., Timonen, H., Saarnio, K., Teinela, K., Karppinen, A., Kukkonen, J., and Hillamo, R.: Chemical composition of aerosols during a major biomass burning episode over northern Europe in spring 2006: Experimental and modelling assessments, *Atmos. Environ.*, 41, 3577–3589, doi:10.1016/j.atmosenv.2006.12.053, 2007.

860 Saarnio, K., Aurela, M., Timonen, H., Saarikoski, S., Teinilä, K., Mäkelä, T., Sofiev, M., Koskinen, J., Aalto, P. P., Kulmala, M., Kukkonen, J., and Hillamo, R.: Chemical composition of fine particles in fresh smoke plumes from boreal wild-land fires in Europe, *Sci. Total Environ.*, 408, 2527–2542, doi:10.1016/j.scitotenv.2010.03.010, 2010.

865 Saxena, P. and Hildemann, L. M.: Water-soluble organics in atmospheric particles: A critical review of the literature and application of thermodynamics to identify candidate compounds, *J. Atmos. Chem.*, 24, 57–109, doi:10.1007/BF00053823, 1996.

Schauer, J. J., Kleeman, M. J., Cass, G. R., and Simoneit, B. R. T.: Measurement of emissions from air pollution sources. 3. C-1–C-29 organic compounds from fireplace combustion of wood, *Environ. Sci. Technol.*, 35, 1716–1728, doi:10.1021/es001331e, 2001.

870 Seinfeld, J. H. and Pandis, S. N.: *Atmospheric Chemistry and Physics*, John Wiley & Sons, New York, 1998.

Semeniuk, T. A., Wise, M. E., Martin, S. T., Russell, L. M., and Buseck, P. R.: Hygroscopic behavior of aerosol particles from biomass fires using environmental transmission electron microscopy, *J. Atmos. Chem.*, 56, 259–273, doi:10.1007/s10874-006-9055-5, 2007.

875 Shantz, N. C., Leaitch, W. R., Phinney, L., Mozurkewich, M., and Toom-Sauntry, D.: The effect of organic compounds on the growth rate of cloud droplets in marine and forest settings, *Atmos. Chem. Phys.*, 8, 5869–5887, doi:10.5194/acp-8-5869-2008, 2008.

Sheffield, A. E., Gordon, G. E., Currie, L. A., and Riederer, G. E.: Organic, elemental, and isotopic tracers of air-pollution sources in Albuquerque, NM, *Atmos. Environ.*, 28, 1371–1384, doi:10.1016/1352-2310(94)90200-3, 1994.

880 Shilling, J. E., King, S. M., Mochida, M., Worsnop, D. R., and Martin, S. T.: Mass spectral evidence that small changes in composition caused by oxidative aging processes alter aerosol CCN properties, *J. Phys. Chem. A*, 111, 3358–3368, doi:10.1021/jp068822r, 2007.

Simoneit, B. R. T.: A review of biomarker compounds as source indicators and tracers for air pollution, *Environ. Sci. Pollut. Res.*, 6, 159–169, doi:10.1007/BF02987621, 1999.

885 Slade, J. H. and Knopf, D. A.: Heterogeneous OH oxidation of biomass burning organic aerosol surrogate compounds: assessment of volatilisation products and the role of OH concentration on the reactive uptake kinetics, *Phys. Chem. Chem. Phys.*, 15, 5898–5915, doi:10.1039/c3cp44695f, 2013.

890 Slade, J. H. and Knopf, D. A.: Multiphase OH oxidation kinetics of organic aerosol: The role of particle phase state and relative humidity, *Geophys. Res. Lett.*, 41, doi:10.1002/2014GL060582, 2014.

Springmann, M., Knopf, D., and Riemer, N.: Detailed heterogeneous chemistry in an urban plume box model: reversible co-adsorption of O₃, NO₂, and H₂O on soot coated with benzo[a]pyrene, *Atmos. Chem. Phys.*, 9, 7461–7479, doi:10.5194/acp-9-7461-2009, 2009.

895 Stocker, T. F., Qin, D., Plattner, G. K., Tignor, M., Allen, S. K., Boschung, J., Nauels, A., Xia, Y., Bex, V., and Midgley, P. M.: *Climate Change 2013: The Physical Science Basis. Contribution of Working Group I to the Fifth Assessment Report of the Intergovernmental Panel on Climate Change*, Cambridge University Press, 2013.

Suda, S. R., Petters, M. D., Yeh, G. K., Strollo, C., Matsunaga, A., Faulhaber, A., Ziemann, P. J., Prenni, A. J., Carrico, C. M., Sullivan, R. C., and Kreidenweis, S. M.: Influence of functional groups on organic aerosol cloud condensation nucleus activity, *Environ. Sci. Technol.*, 48, 10 182–10 190, doi:10.1021/es502147y, 900 2014.

Svenningsson, B., Rissler, J., Swietlicki, E., Mircea, M., Bilde, M., Facchini, M. C., Decesari, S., Fuzzi, S., Zhou, J., Monster, J., and Rosenorn, T.: Hygroscopic growth and critical supersaturations for mixed aerosol particles of inorganic and organic compounds of atmospheric relevance, *Atmos. Chem. Phys.*, 6, 905 1937–1952, doi:10.5194/acp-6-1937-2006, 2006.

Timonen, H., Carbone, S., Aurela, M., Saarnio, K., Saarikoski, S., Ng, N. L., Canagaratna, M. R., Kulmala, M., Kerminen, V. M., Worsnop, D. R., and Hillamo, R.: Characteristics, sources and water-solubility of ambient submicron organic aerosol in springtime in Helsinki, Finland, *J. Aero. Sci.*, 56, 61–77, doi:10.1016/j.jaerosci.2012.06.005, 2013.

910 van der Werf, G. R., Randerson, J. T., Giglio, L., Collatz, G. J., Kasibhatla, P. S., and Arellano Jr, A. F.: Interannual variability in global biomass burning emissions from 1997 to 2004, *Atmos. Chem. Phys.*, 6, 3423–3441, doi:10.5194/acp-6-3423-2006, 2006.

Vingarzan, R.: A review of surface ozone background levels and trends, *Atmos. Environ.*, 38, 3431–3442, doi:10.1016/j.atmosenv.2004/03.030, 2004.

915 Wang, B. and Knopf, D. A.: Heterogeneous ice nucleation on particles composed of humic-like substances impacted by O₃, *J. Geophys. Res.*, 116, D03 205, doi:10.1029/2010JD014964, 2011.

Wang, B., Laskin, A., Roedel, T., Gilles, M. K., Moffet, R. C., Tivanski, A., and Knopf, D. A.: Heterogeneous ice nucleation and water uptake by field-collected atmospheric particles below 273 K, *J. Geophys. Res.*, 117, D00V19, doi:10.1029/2012JD017446, 2012.

920 Wang, J., Lee, Y.-N., Daum, P. H., Jayne, J., and Alexander, M. L.: Effects of aerosol organics on cloud condensation nucleus (CCN) concentration and first indirect aerosol effects, *Atmos. Chem. Phys.*, 8, 6325–6339, doi:10.5194/acp-8-6325-2008, 2008.

Wong, J. P. S., Lee, A. K. Y., Slowik, J. G., Cziczo, D. J., Leaitch, W. R., Macdonald, A., and Abbatt, J. P. D.: Oxidation of ambient biogenic secondary organic aerosol by hydroxyl radicals: effects on cloud 925 condensation nuclei activity, *Geophys. Res. Lett.*, 38, L22 805, doi:10.1029/2011GL049351, 2011.

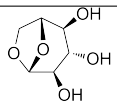
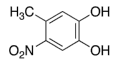
Zhang, Q., Jimenez, J. L., Canagaratna, M. R., Allan, J. D., Coe, H., Ulbrich, I., Alfarra, M. R., Takami, A., Middlebrook, A. M., Sun, Y. L., Dzepina, K., Dunlea, E., Docherty, K., DeCarlo, P. F., Salcedo, D., Onasch, T., Jayne, J. T., Miyoshi, T., Shimojo, A., Hatakeyama, S., Takegawa, N., Kondo, Y., Schneider, J., Dewnack, F., Borrmann, S., Weimer, S., Demerjian, K., Williams, P., Bower, K., Bahreini, R., Cottrell, 930 L., Griffin, R. J., Rautiainen, J., Sun, J. Y., Zhang, Y. M., and Worsnop, D. R.: Ubiquity and dominance

of oxygenated species in organic aerosols in anthropogenically-influenced Northern Hemisphere midlatitudes, *Geophys. Res. Lett.*, 34, L13 801, doi:10.1029/2007GL029979, 2007.

Zhao, R., Mungall, E. L., Lee, A. K. Y., Aljawhary, D., and Abbatt, J. P. D.: Aqueous-phase photooxidation of levoglucosan - a mechanistic study using Aerosol Time of Flight Chemical Ionization Mass Spectrometry (Aerosol-ToF-CIMS), *Atmos. Chem. Phys.*, 14, 9695–9706, doi:10.5194/acp-14-9695-2014, 2014.

935

Table 1. Chemical properties of the different particle types investigated in this study and the parameters used in predicting κ .

Molecule	Structure	M (g mol ⁻¹)	ρ (g cm ⁻³)	Solubility (g L ⁻¹)	C_i	ν
Levoglucosan		162.14	1.69	1000	0.592	1
4-methyl-5-nitrocatechol		169.13	1.5	6	0.004	1
K ₂ SO ₄		174.26	2.66	11	0.042	2 ^a

^aTaken from the reported Van't Hoff factor in Low (1969) for (NH₄)₂SO₄ assuming a solution droplet molality of approximately 0.2.

Table 2. Tabulated hygroscopicity parameters, κ , for the various particle types investigated in this study.

Compound	κ^1	κ^2	κ^3	References
Levogluconan	0.169 (± 0.013)	0.188	0.165	Carrico et al. (2010)
			0.208 (± 0.015)	Petters and Kreidenweis (2007)
K ₂ SO ₄	0.55 (± 0.08)	0.55	0.52	Carrico et al. (2010)
4-methyl-5-nitrocatechol	0.009 (± 0.005) ^a	0.16		
LEV:MNC:KS mass ratio	κ^1	κ^2	κ^4	
1:1:0	0.131 (± 0.014)	0.173	0.085	
1:0:1	0.355 (± 0.042)	0.329	0.318	
0:1:1	0.301 (± 0.047)	0.300	0.204	
1:1:1	0.261 (± 0.012)	0.256	0.188	
1:0.03:0.3	0.227 (± 0.016)	0.241	0.221	

¹This study. Reported uncertainties are 1 σ from the mean in the measured κ . ²Predicted values applying the volume mixing rule without solubility limitations. ³Literature reported values. ⁴Predicted values applying the volume mixing rule and experimentally derived single-component κ (i.e. with solubility limitations).

^a Apparent κ from κ -lookup table taken from <http://www4.ncsu.edu/mdpetter/code.html>.

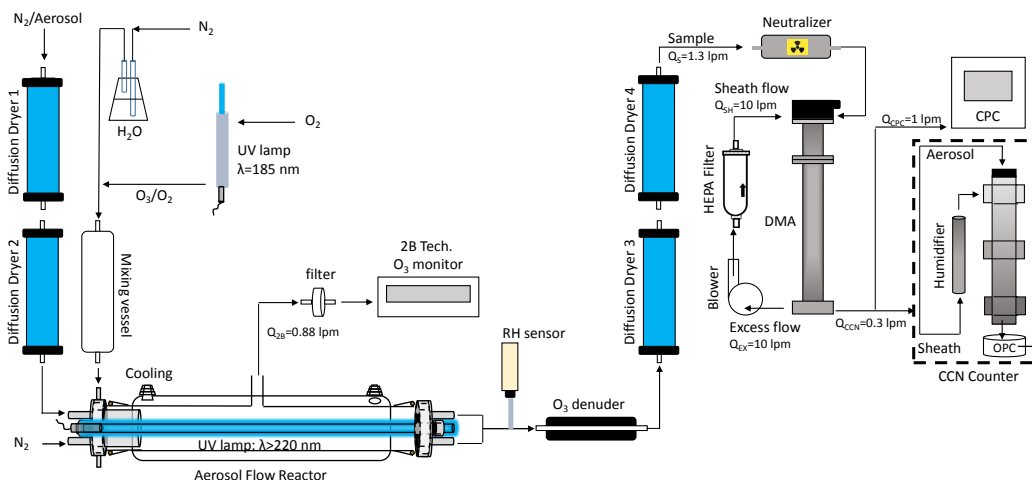


Figure 1. Schematic illustration of the experimental setup to examine the effect of OH and O₃ oxidation on the CCN activity of single-component and multicomponent biomass burning aerosol surrogate-particles. From top left to bottom right: aerosol generation and drying stage, O₃ production and humidification (mixing vessel), the aerosol flow reactor, O₃-free ultra-violet lamp and O₃ monitor, relative humidity probe (RH sensor), O₃ denuder, second drying stages, aerosol sizing by the DMA and particle counting by the CPC, and determination of the CCN activity by the CCNc.

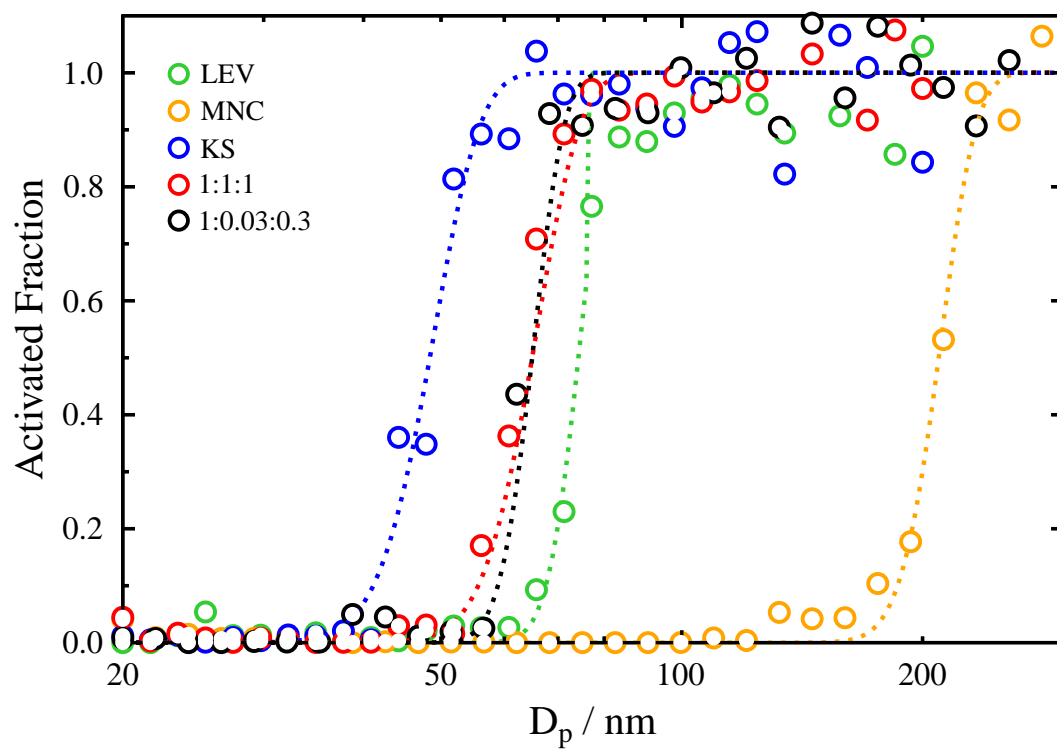


Figure 2. Activated fractions, i.e. fraction of the number of particles at a given particle size activated to CCN as a function of the initial dry particle diameter, for LEV (green), MNC (orange), KS (blue), 1:1:1 (red) and 1:0.03:0.3 (black) particles at a $S=0.425\%$. The dotted lines correspond to the fits applying Eq. 8.

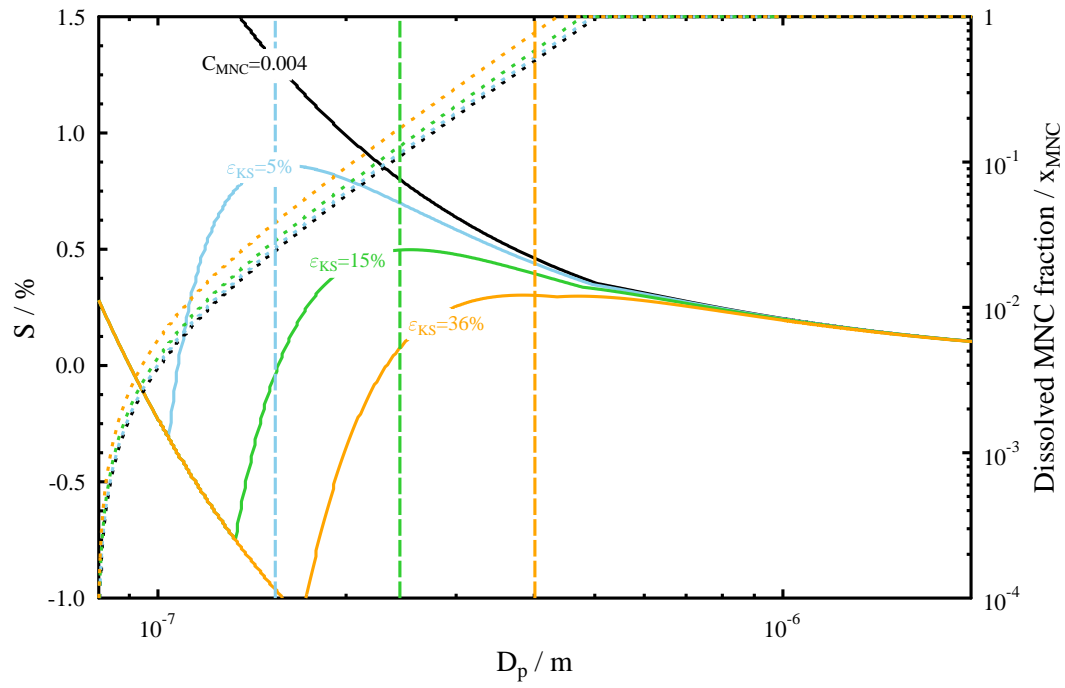


Figure 3. Example Köhler curves (solid lines) calculated from Eq. 1 for pure MNC (black), MNC mixed with 5% (blue), 15% (green), and 36% (orange) by volume KS. The dotted lines are the dissolved fractions of MNC, x_{MNC} , calculated from Eq. 7, corresponding to the different Köhler curves. The vertical dashed lines indicate the maxima of the different Köhler curves.

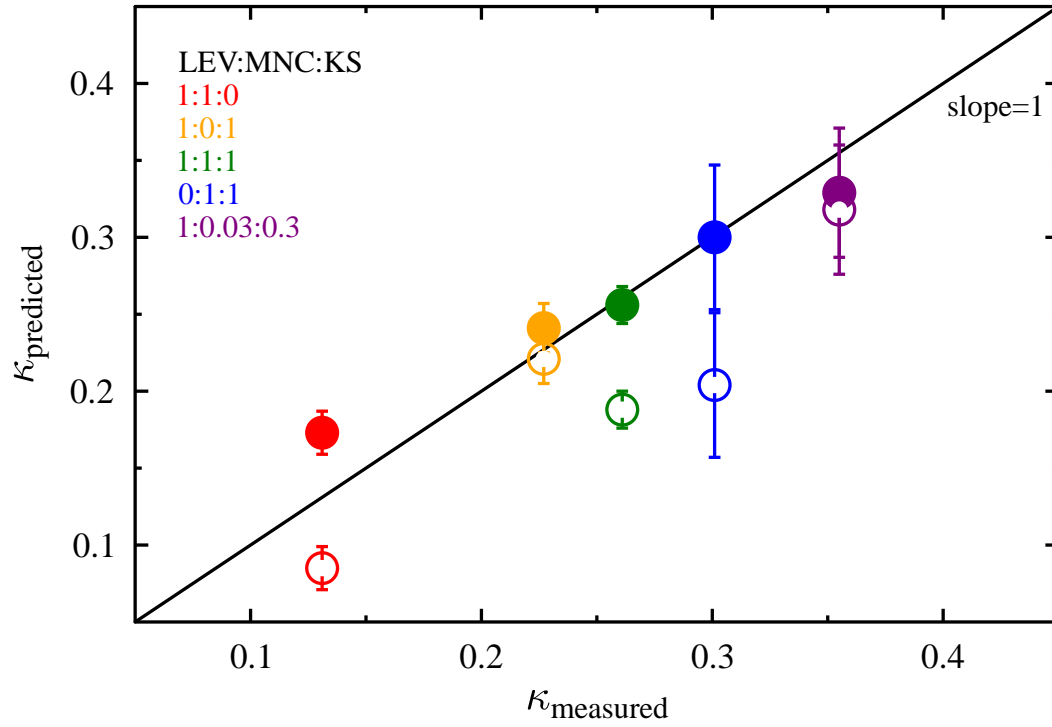


Figure 4. Measured κ values for the binary and ternary particle mixtures of LEV, MNC, and KS, shown as a function of predicted κ applying the volume mixing rule including solubility limitations (open circles) and excluding solubility limitations (closed circles). The black line represents a slope of 1 in the measured versus predicted κ . The LEV:MNC:KS mass ratios are indicated in the legend for 1:1:0 (red), 1:0:1 (orange), 1:1:1 (green), 0:1:1 (blue), and 1:0.03:0.3 (purple). See text for more details.

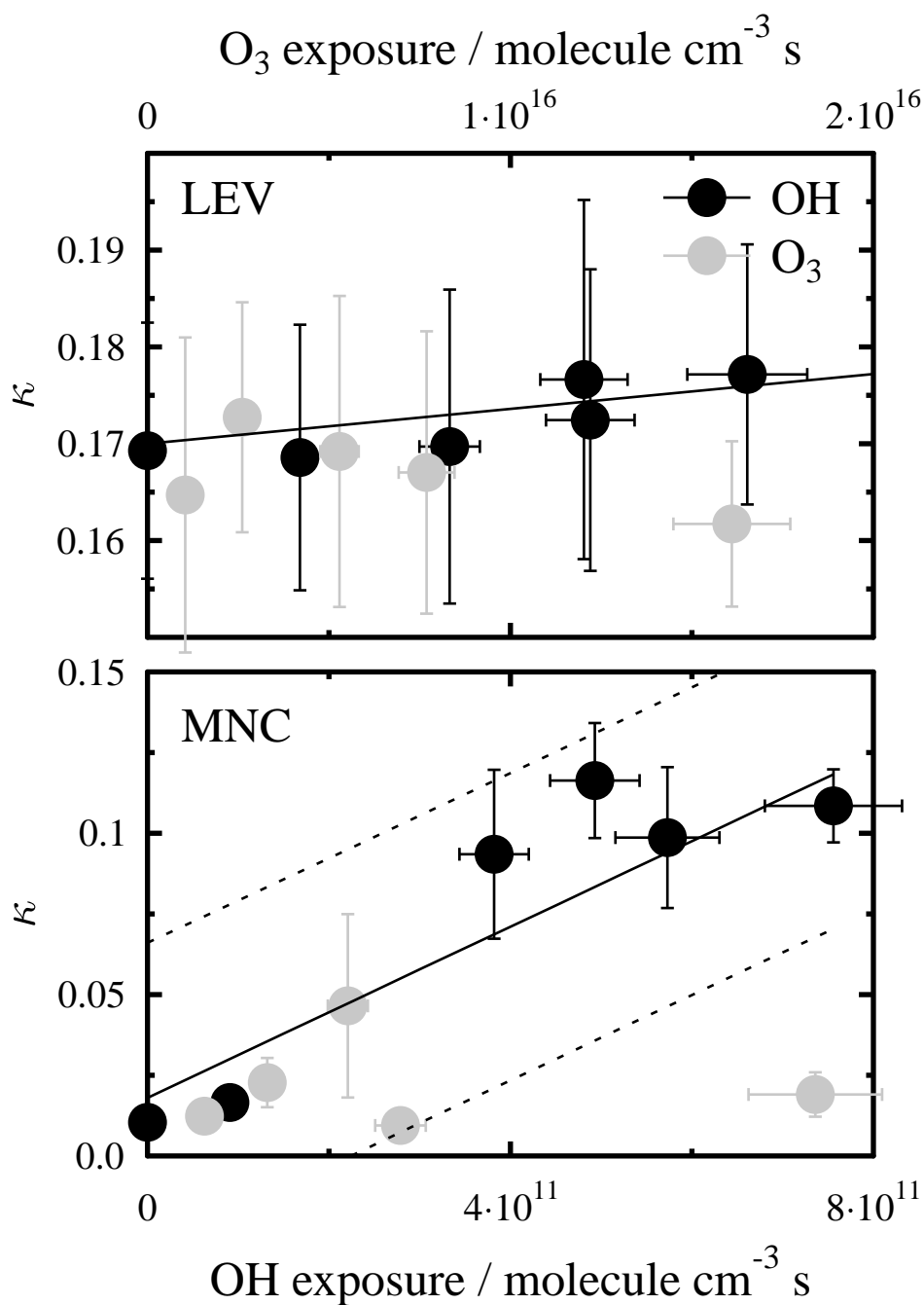


Figure 5. Derived κ for LEV and MNC particles are shown as a function of OH and O_3 exposure. The black circles correspond to κ due to chemical aging by OH and the gray circles correspond to κ due to chemical aging by O_3 . The vertical error bars represent $\pm 1\sigma$ from the mean of the data acquired at a given OH or O_3 exposure. Horizontal error bars of the κ values correspond to the uncertainty in the OH exposure based on a $\pm 5\%$ drift in RH over the sampling period. Horizontal error bars of the κ for the O_3 exposures correspond to the uncertainty in the O_3 exposure based on a drift in the measured $[O_3]$ of $\pm 10\%$. The solid black lines show the best linear fit to the OH exposure data and the dashed lines in the lower panel show the 95% confidence intervals of the fit.

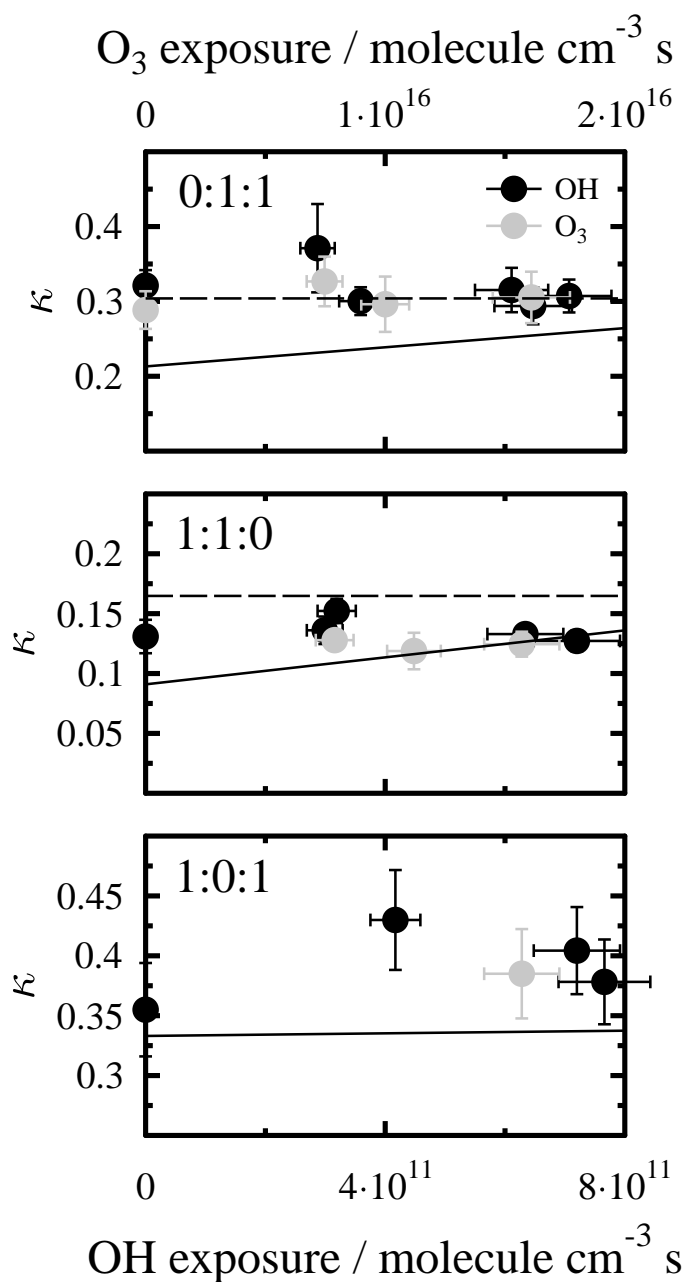


Figure 6. Derived κ for the binary component particles with LEV:MNC:KS mass ratios 0:1:1 (top), 1:1:0 (middle), and 1:0:1 (bottom) are shown as a function of OH and O_3 exposure. The black circles correspond to κ due to chemical aging by OH and the gray circles correspond to κ due to chemical aging by O_3 . Error bars are same as given in Fig. 5. The solid black lines are modeled κ using the volume mixing rule as a function of OH exposure including MNC solubility limitations and applying the linear fit to the measured κ of pure MNC as a function of OH exposure (Fig. 5). The dashed lines are modeled κ using the volume mixing rule as a function of OH exposure excluding MNC solubility limitations.

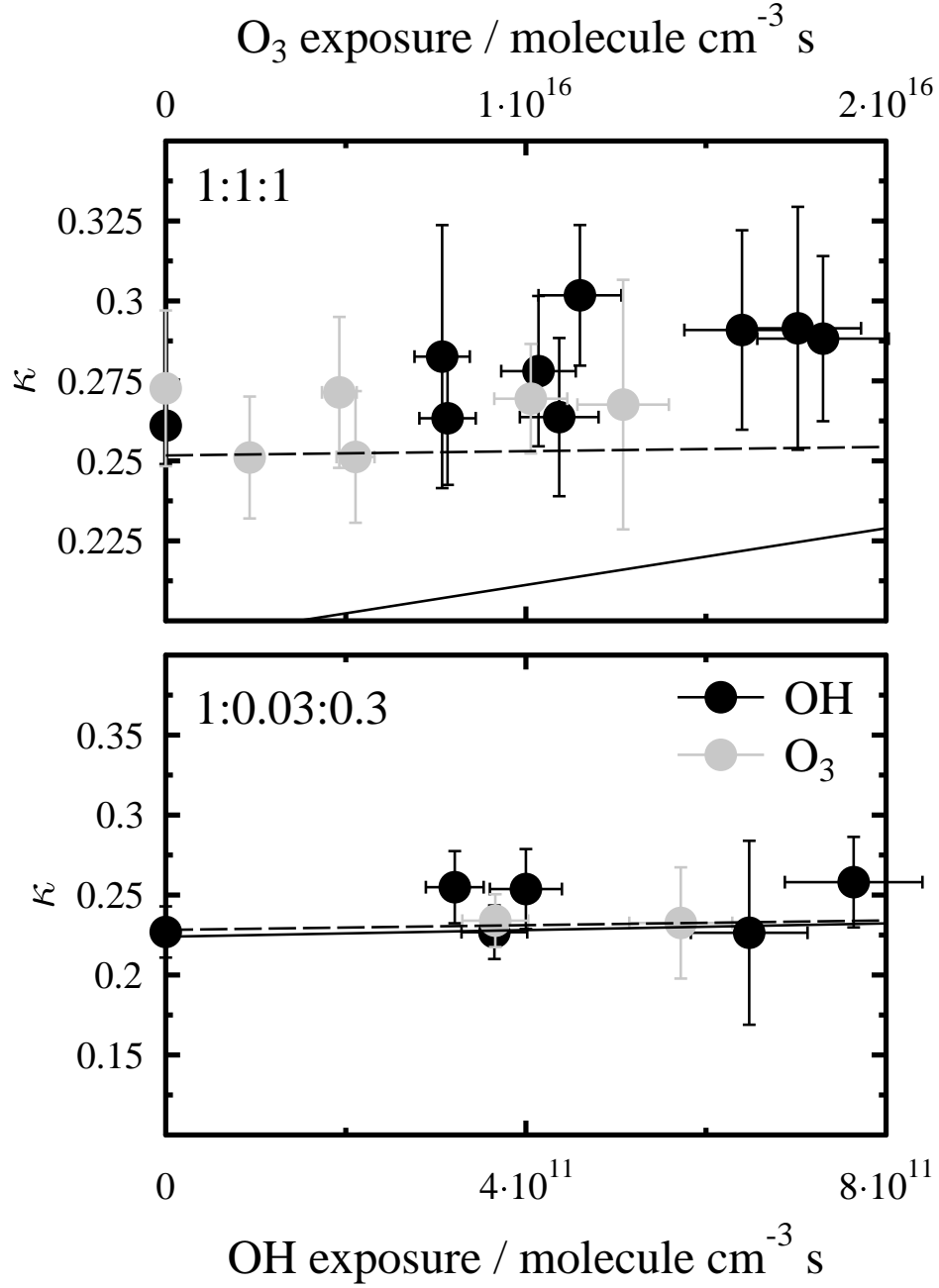


Figure 7. Derived κ for the ternary component particles with LEV:MNC:KS mass ratios 1:1:1 (top) and 1:0.03:0.3 (bottom) are shown as a function of OH and O_3 exposure. The black circles correspond to κ due to chemical aging by OH and the gray circles correspond to κ due to chemical aging by O_3 . Error bars and dashed lines are same as given in Figs. 5 and 6, respectively.

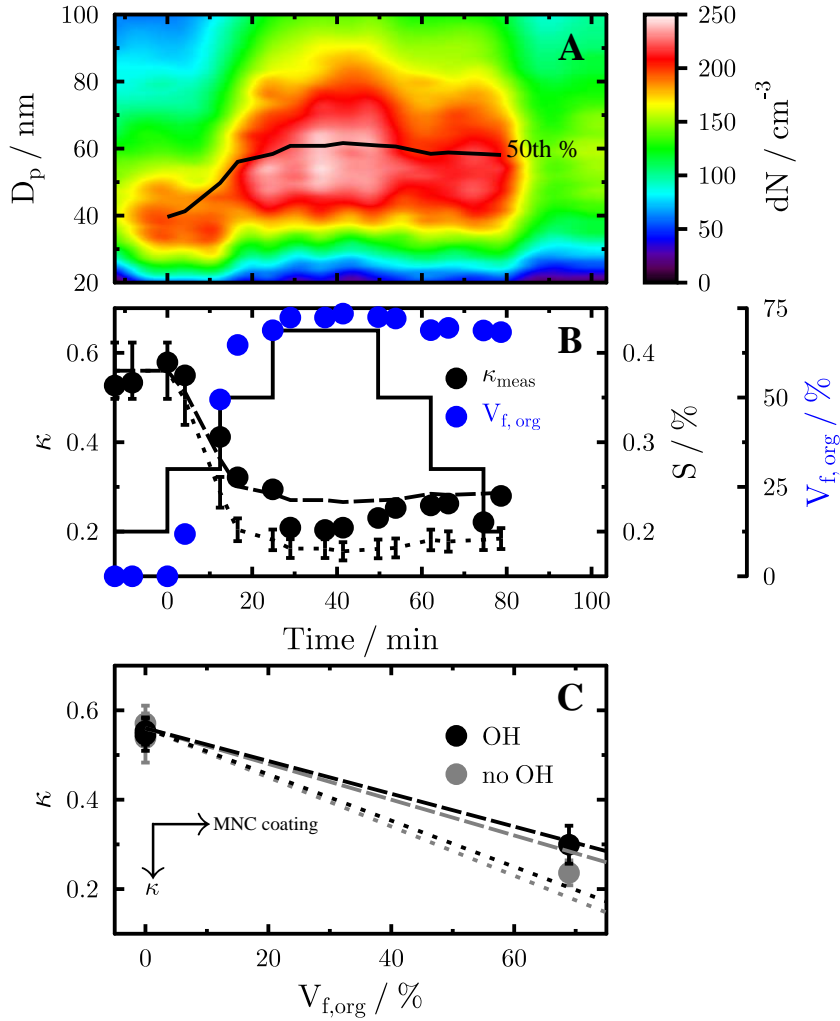


Figure 8. OH exposure effects on the CCN activity of MNC-coated KS particles. Panel A shows a color map of the number-weighted particle size distribution (dN) of KS and MNC-coated KS particles plotted as a function of MNC-coating. Panel B displays the change in particle hygroscopicity (black circles) and MNC volume fraction ($V_{f,org}$, blue circles) with time as a function of S given as black solid line. The dotted line shows the predicted κ using the volume mixing rule corresponding to the $V_{f,org}$ at a given time and assuming the CCN activity of MNC is limited by its solubility (i.e. $MNC \kappa = 0.009(\pm 0.005)$). The dashed line presents the predicted κ using the volume mixing rule corresponding to the $V_{f,org}$ at a given time and assuming the CCN activity of MNC is not limited by its solubility (i.e. $MNC \kappa = 0.16$ calculated from Eq. 6). Panel C displays the change in κ for the MNC-coated KS particles as a function of $V_{f,org}$ and OH exposure. OH unexposed particles are plotted as gray circles. Particles exposed to OH at $3.3 \times 10^{11} \text{ molecule cm}^{-3} \text{ s}$ are represented by black circles. The error bars represent 1σ from the mean in κ . The dotted lines show predicted κ using the volume mixing rule assuming the CCN activity of MNC is limited by its solubility for the unexposed (gray) and OH exposed (black) particles. The dashed lines show predicted κ using the volume mixing rule assuming the CCN activity of MNC is not limited by its solubility for the unexposed (gray) and OH exposed (black) particles.